A 3D ribbon diagram of a protein structure, rendered in white. The protein is complex, with several alpha-helices and beta-sheets. Some regions are highlighted in different colors: a large green area in the center, a yellow area on the right, and a red area at the bottom. The background is a light gray.

**The architecture of native, reconstituted
and artificial light-harvesting molecular
(macro-)assemblies – as revealed by
polarization spectroscopic and
microscopic techniques**

Győző Garab
**Biological Reserach Centre, Hungarian Academy of
Sciences, Szeged, Hungary**

Acknowledgements

Biological Research Centre Szeged

- Petar Lambrev
- Gábor Steinbach
- Yuliya Miloslavina
- Krzysztof Pawlak
- István Pomozi
- Zsuzsanna Várkonyi
- Parveen Akhtar

Max-Planck Institute, Mülheim

Alfred R. Holzwarth and coworkers

Institute of Botany, CAS, Beijing

Chunhong Yang and coworkers

Aix-Marseille Univ., Marseille

Silviu T. Balaban and coworkers

Nanyang Techn. Univ., Singapore

Howe-Siang Tan and coworkers

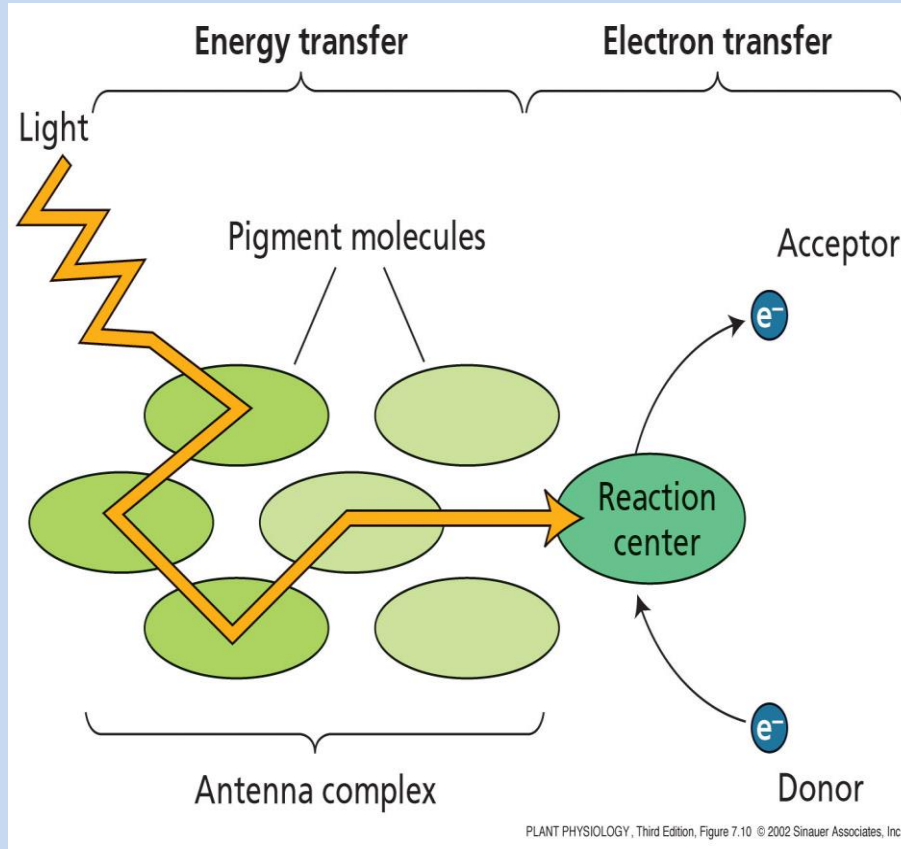
Technical University, Berlin

Gernot Renger and coworkers

In this talk:

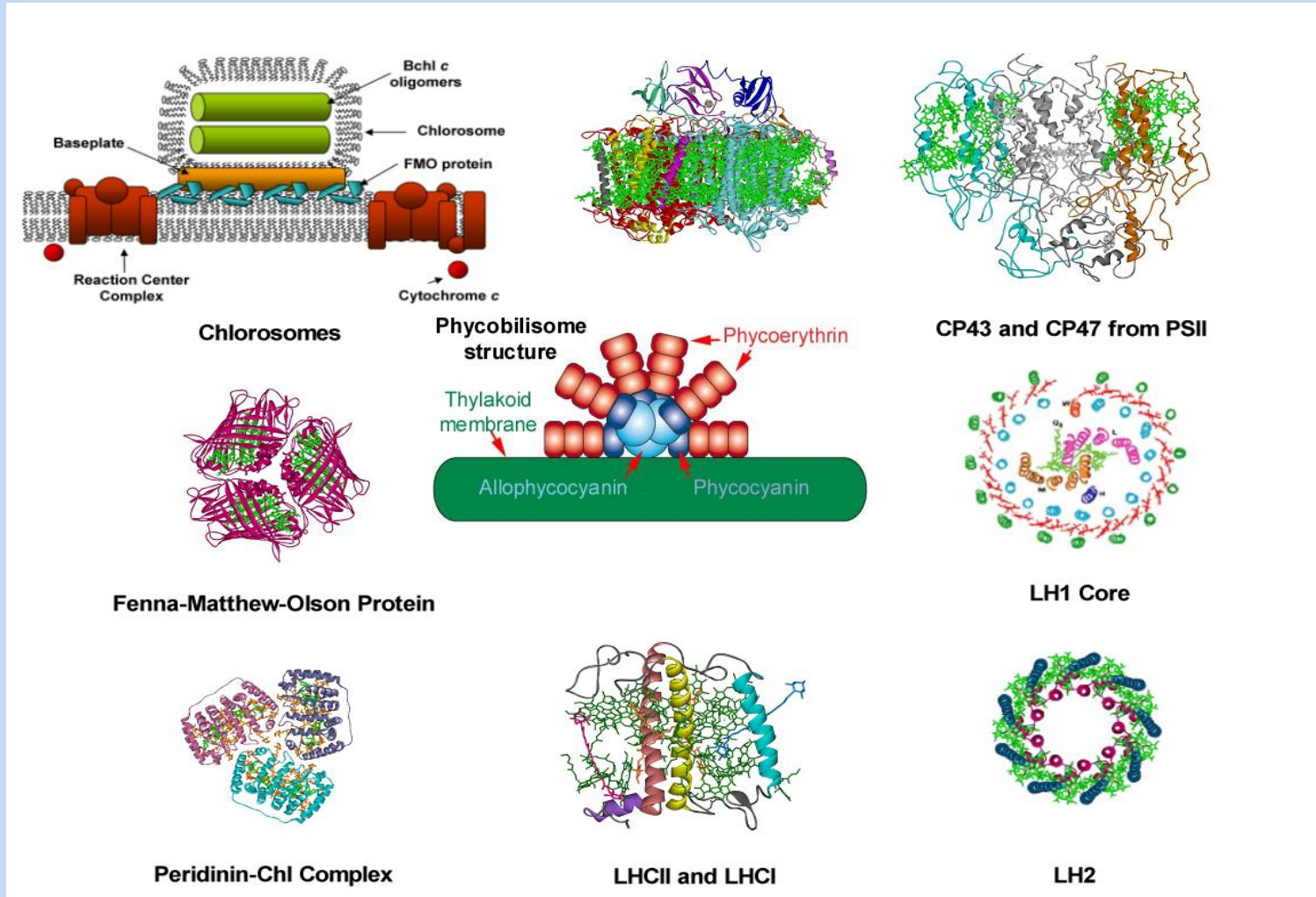
- Light-harvesting antennae in photosynthetic organisms
- Non-random orientation of the pigment molecules – linear dichroism spectroscopy
- Pigment-pigment (short-range) excitonic interactions and extended arrays of the chromophores with long-range order – circular dichroism spectroscopy techniques
- The migration of the excitation energy in LHCII - 2D spectroscopy, and in larger arrays – effective domain sizes
- ‚Artificial chlorosome‘
- Microscopic order and micromanipulation of anisotropic particles

Light-harvesting antennae



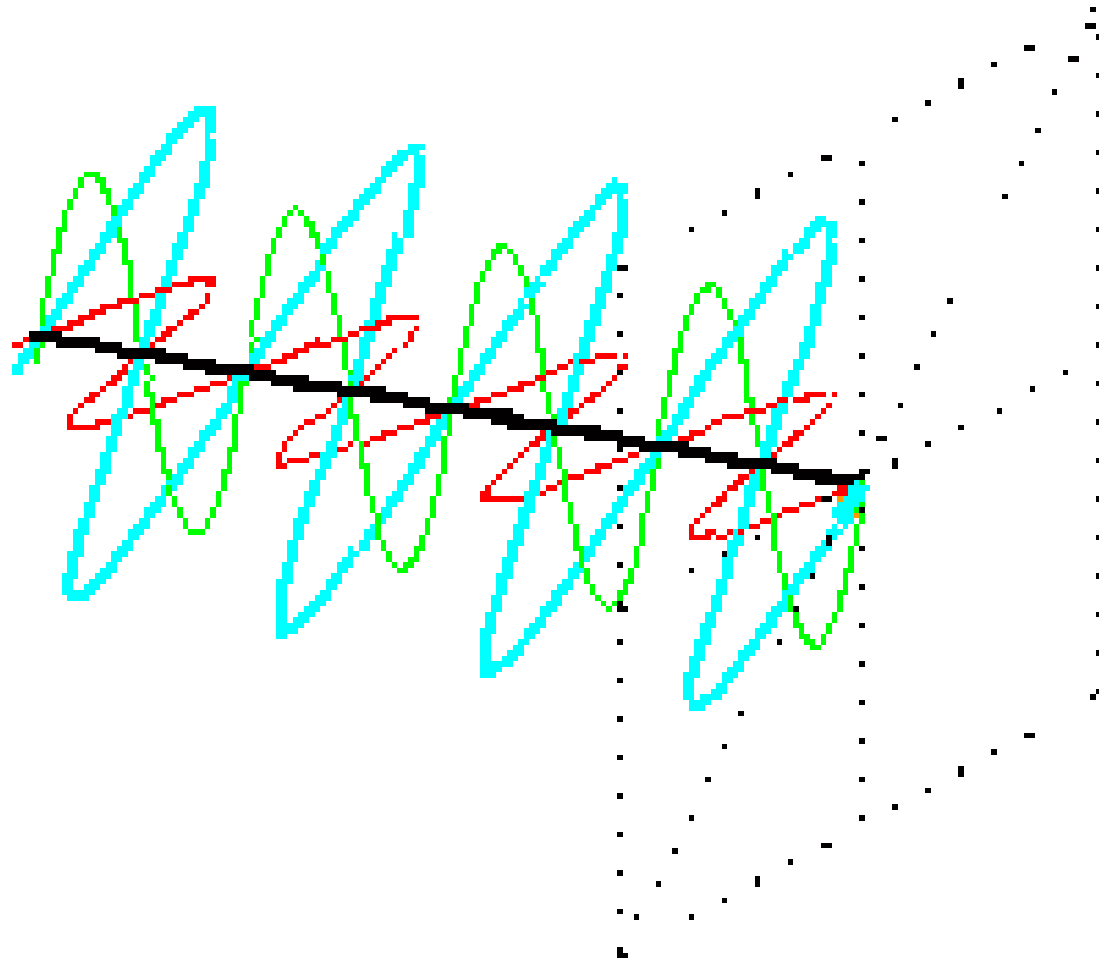
- ▶ Absorption of light and excitation energy transfer to the Reaction Center (RC)
- ▶ Increases the effective absorption cross-section.
- ▶ Important role in photoadaptation of photosynthetic organisms to the environment.

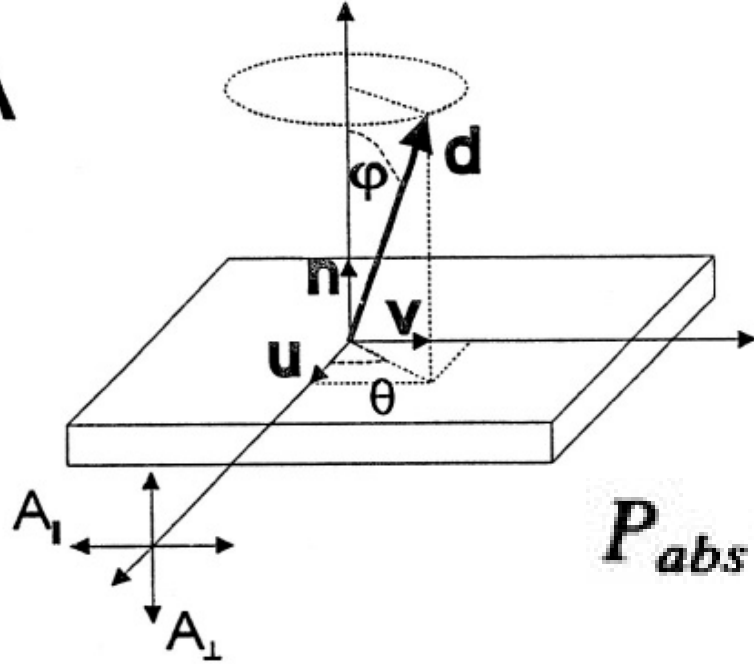
Antenna Complexes



Extreme diversity of antenna systems strongly suggests multiple independent evolutionary origins

Linearly polarized light

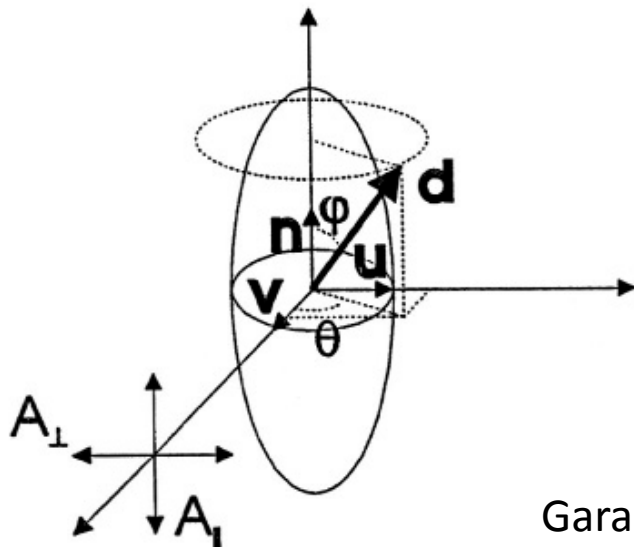


A**LD**

basic principle and
definition

$$P_{abs} \sim (\mathbf{E} \cdot \boldsymbol{\mu})^2 = E^2 \mu^2 \cos^2 \alpha$$

$$LD \equiv A_{\parallel} - A_{\perp} = \frac{3}{2} A (1 - 3 \cos^2 \varphi)$$

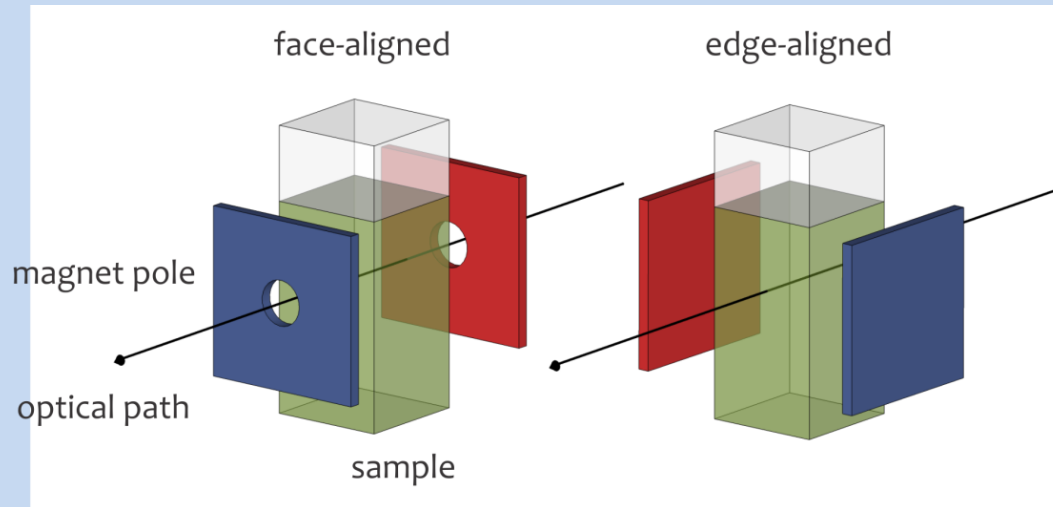
B

Orientation parameter:
 $S = LD/3A$

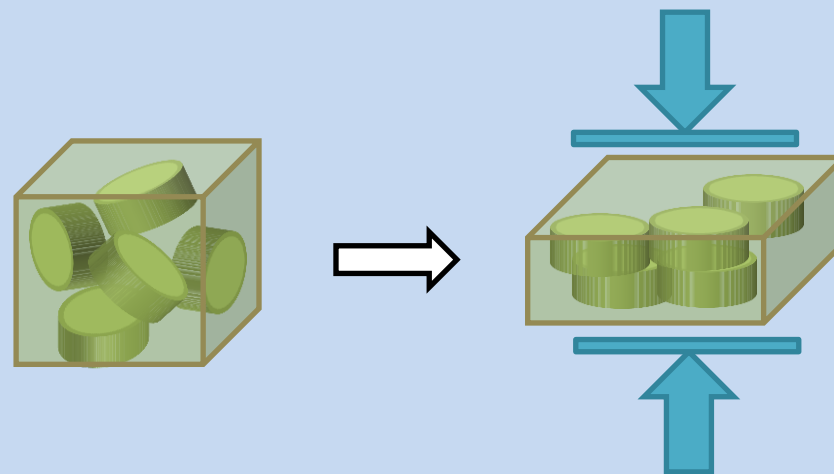
Also, polarized fluorescence emission

Garab, in Biophysical Techniques in Photosynthesis, Kluwer, 1996

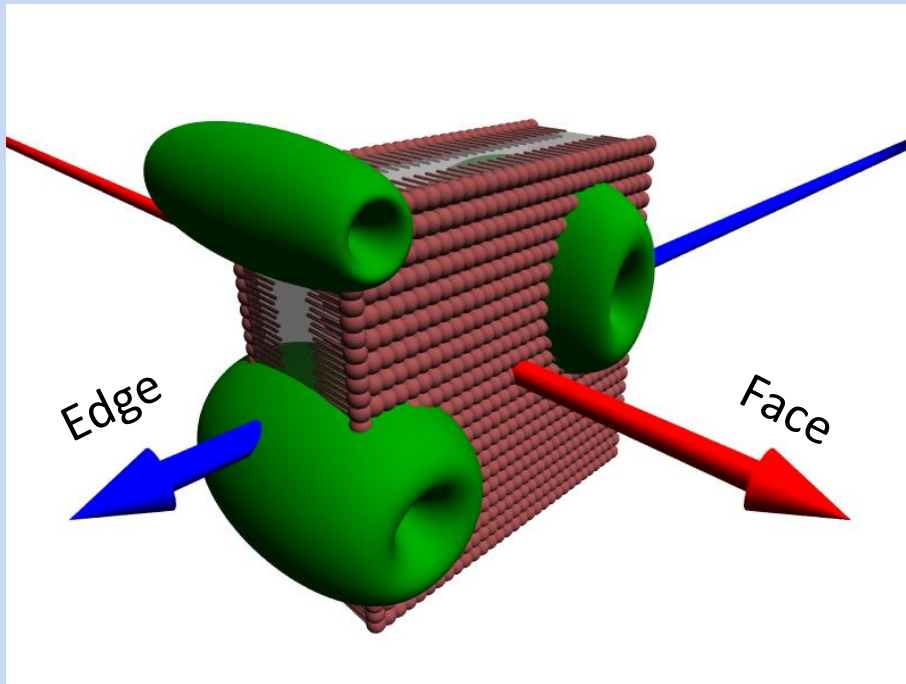
Sample Orientation (Alignment)



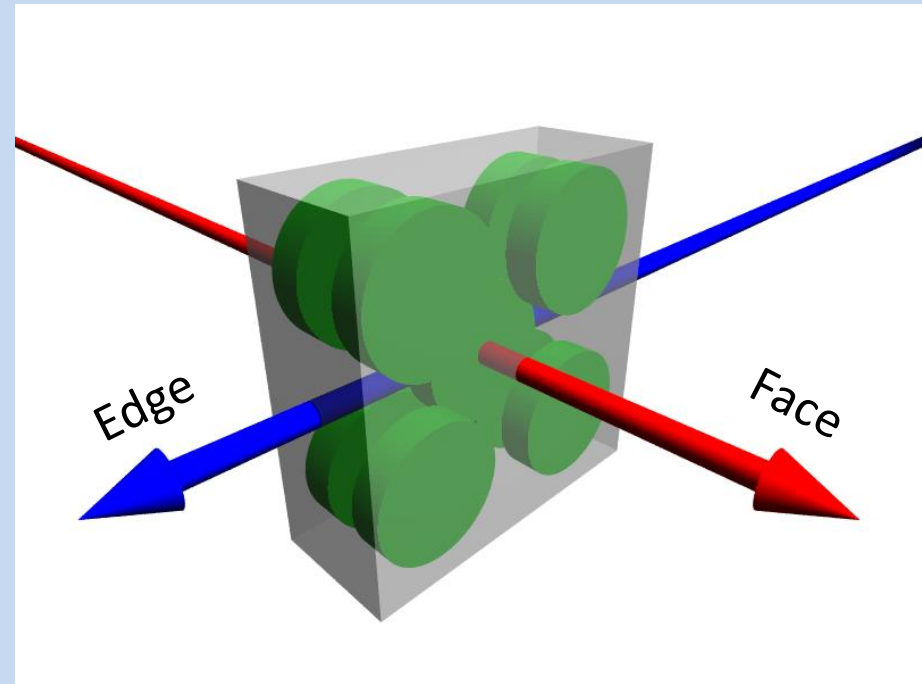
Magnetic orientation



Orientation of membranes

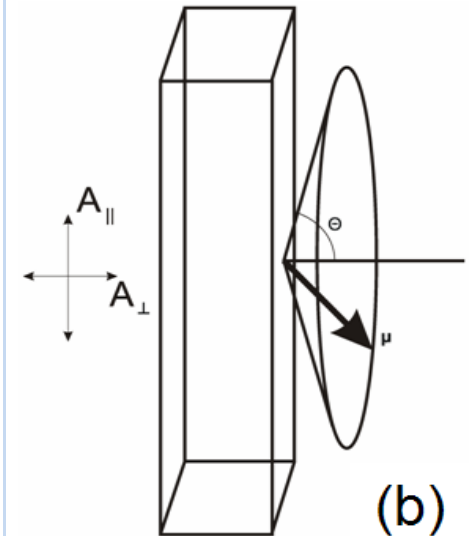
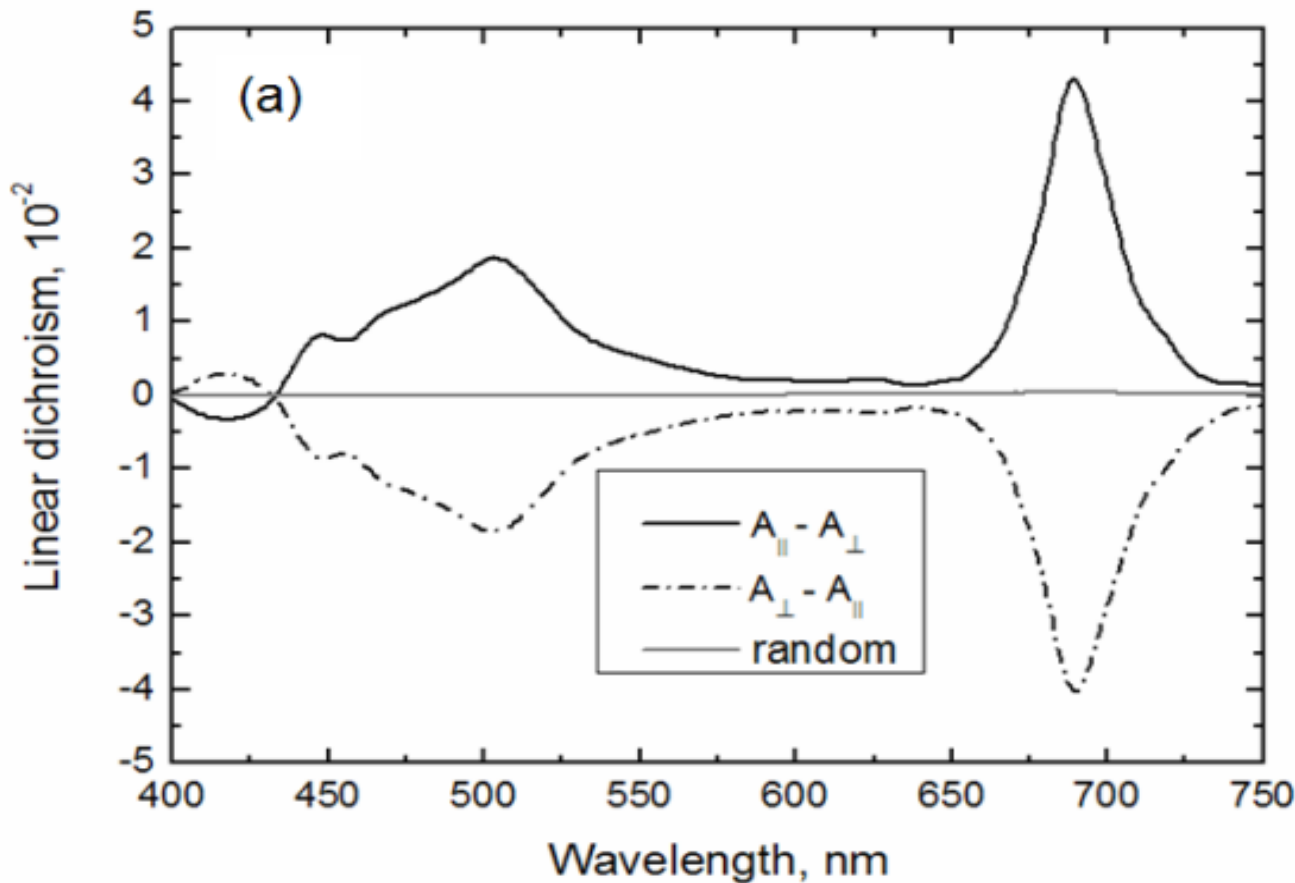


Face-aligned orientation should preferentially excite transitions in the membrane plane



Edge-aligned orientation shows transitions primarily perpendicular to the membrane.

LD of magnetically aligned thylakoid membranes, trapped in gel



Förster resonance interaction

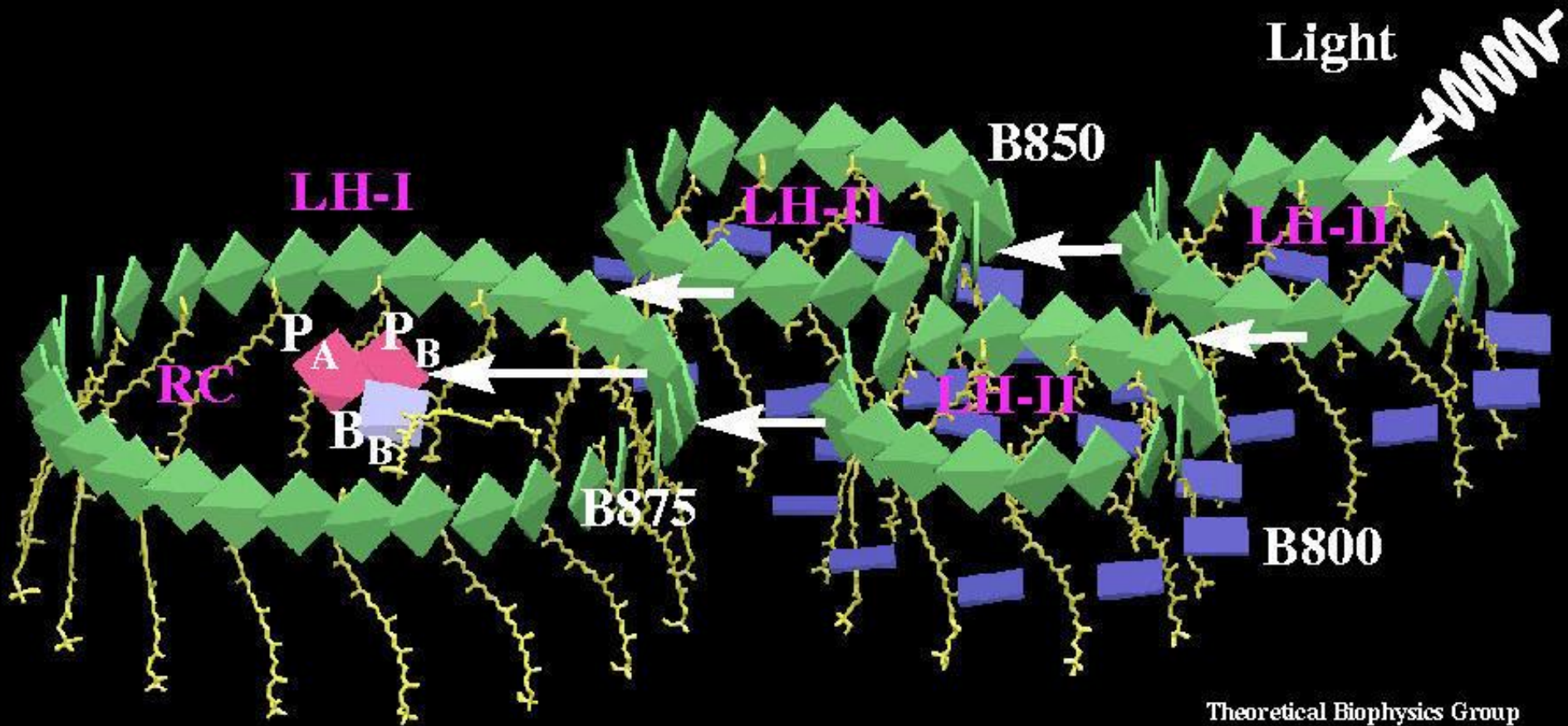
- Coulombic dipole-dipole interaction

$$V_{DA} = \frac{1}{4\pi\epsilon_0 n^2} \frac{\hat{\mu}_D \hat{\mu}_A}{R_{DA}^3} - 3 \frac{(\hat{\mu}_A \hat{R}_{DA})(\hat{\mu}_D \hat{R}_{DA})}{R_{DA}^5}$$

- The rate of energy transfer depends on the mutual orientation of the donor (D) and acceptor molecules (dipoles)

$$k_{DA} = \frac{2\pi}{\hbar} |V_{DA}|^2 J_{DA}$$

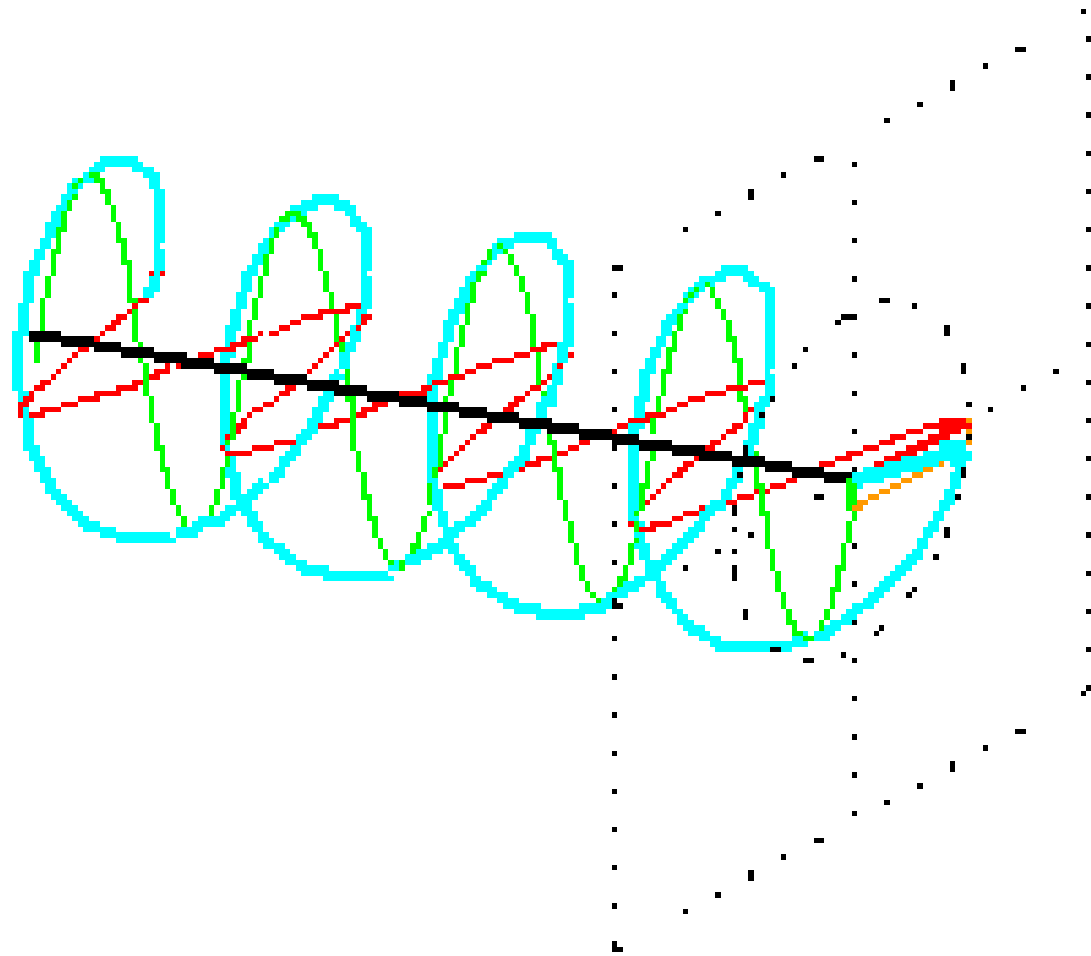
$$J_{DA} = \int_0^\infty f_D(\lambda) \epsilon_A(\lambda) \lambda^4 d\lambda$$



Theoretical Biophysics Group
Beckman Institute
University of Illinois Urbana-Champaign

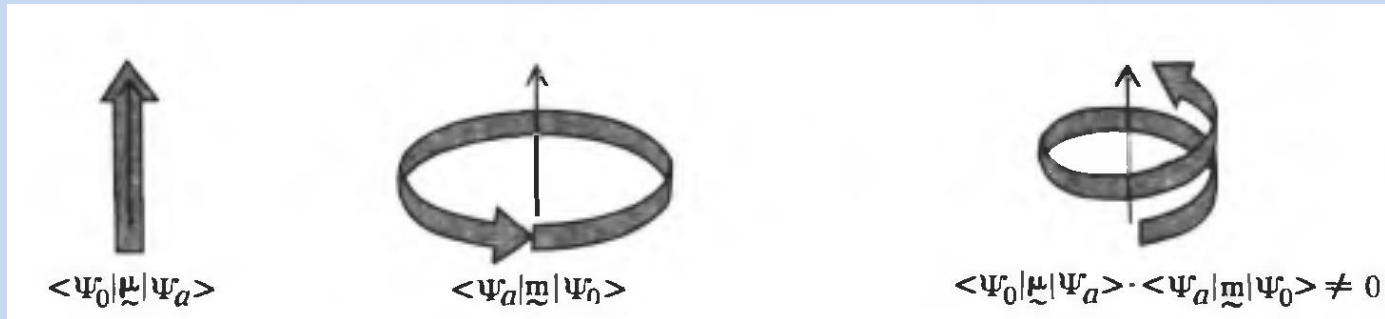
The non-random orientation of the chromophores / pigment molecules (dipoles) appears to be a universal property in photosynthetic system - it has a functional role in determining the excitation energy migration

Circularly polarized light



Physical origins of CD

Molecular charge motions induced by light



Interaction
with the
electric
component

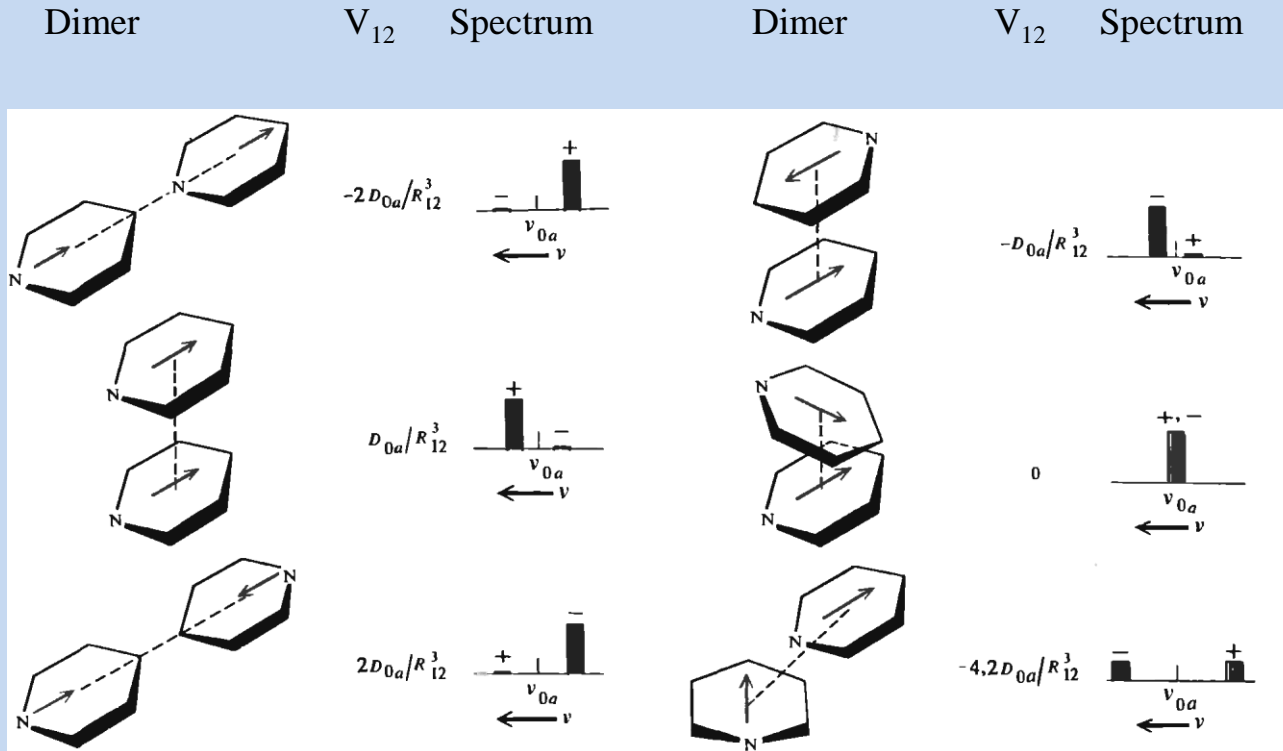
Interaction
with the
magnetic
component

Optical
activity

$$R_{CD} = -\text{Im}(\mu, m)$$

Cantor C.R. & Schimmel P.R., Biophysical Chemistry, 1980, Freeman & Co.

Excitonic coupling



Cantor C.R. & Schimmel P.R., Biophysical Chemistry, 1980, Freeman & Co.

$$\mathcal{R}_{\pm CD} = \pm 1.7 \times 10^{-5} \nu_0 \mu^2 R (\mathbf{r} \cdot \mathbf{d}_2 \times \mathbf{d}_1) \quad \text{Short-range, dipole-dipole-interactions}$$

see also Garab, 1996 in Biophysical Techniques ...

In large, densely packed ordered, so-called psi-type aggregates the electric field at any point is the superposition of the incident electric field and the sum of the fields produced by all oscillating dipoles - thus the CD is more complex, and is an attribute of the entire, highly organized macroaggregate (or the chiral macrodomains)

$$E_{dipole_i} = 4\pi k^2 \Gamma(\mathbf{x}, \mathbf{x}') \cdot \boldsymbol{\mu}_i$$

$$E(\mathbf{x}) = E_0(\mathbf{x}) + \sum_i E_{dipole_i}(\mathbf{x})$$

$$\Gamma(\mathbf{x}, \mathbf{x}') = (3\hat{\mathbf{r}}\hat{\mathbf{r}} - 1) \frac{e^{ikr}}{4\pi k^2 r^3} - (3\hat{\mathbf{r}}\hat{\mathbf{r}} - 1) \frac{ie^{ikr}}{4\pi k r^2}$$

$$+ (1 - \hat{\mathbf{r}}\hat{\mathbf{r}}) \frac{e^{ikr}}{4\pi r} - \frac{1}{3k^2} \delta^3(r)$$

$$\Gamma(\mathbf{x}, \mathbf{x}') = (3\hat{\mathbf{r}}\hat{\mathbf{r}} - 1) \frac{e^{ikr}}{4\pi k^2 r^3} - (3\hat{\mathbf{r}}\hat{\mathbf{r}} - 1) \frac{ie^{ikr}}{4\pi k r^2} + (1 - \hat{\mathbf{r}}\hat{\mathbf{r}}) \frac{e^{ikr}}{4\pi r} - \frac{1}{3k^2} \delta^3(r)$$

Keller and Bustamante, 1986, J Chem Phys

See also Garab 1996; Garab and van Amerongen, 2009 – and the references therein

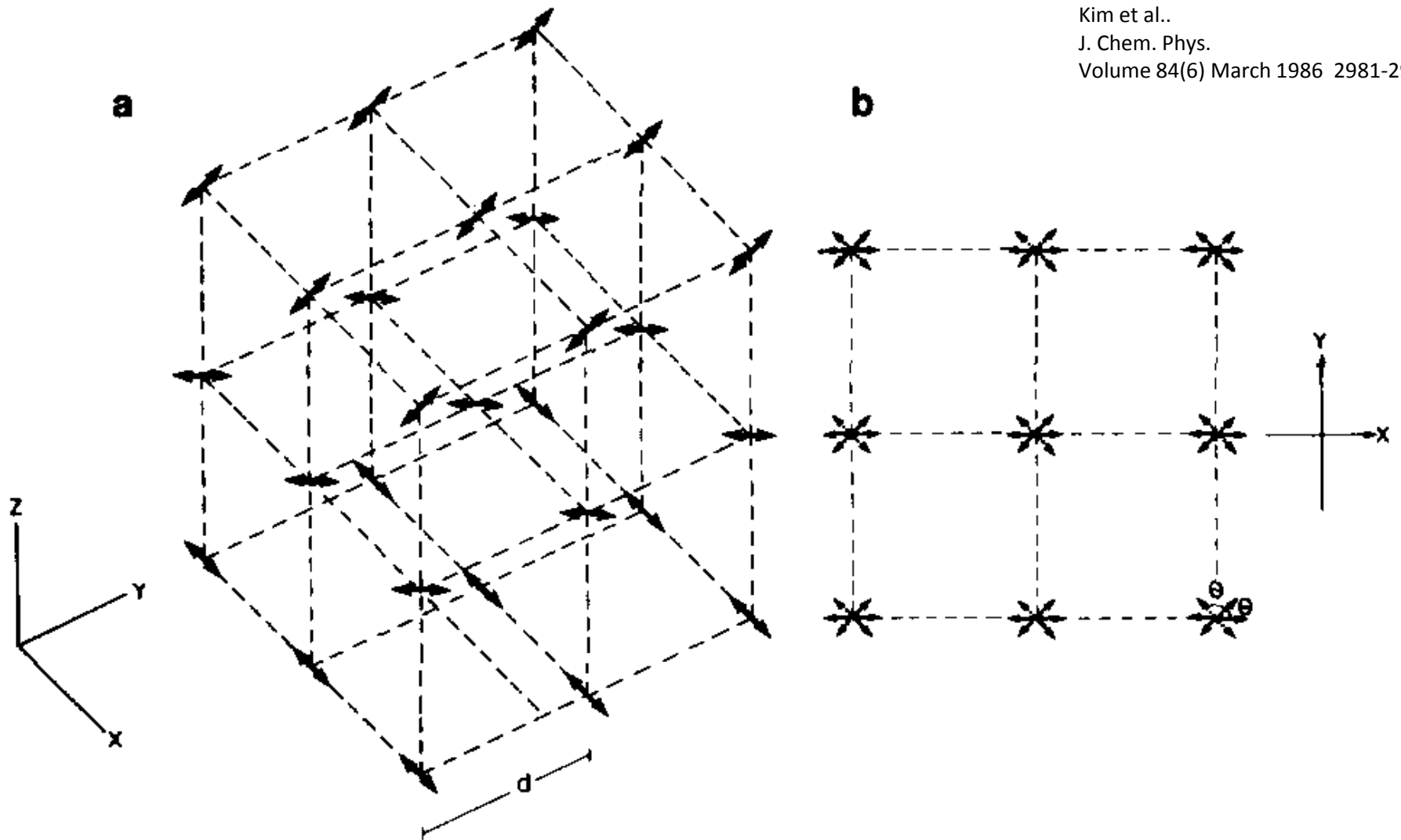


FIGURE 2 Geometry for the psi-type CD calculations: (a) 27 uniaxial polarizable axes with only xy components are situated on the cubic lattice points and each layer is twisted an angle, θ , which determines the pitch of the model system. d is the distance between the polarizable groups on each coordinate. Each polarizable axis represents the volume of d^3 . Therefore, the volume which these 27 polarizable axes represent is $(3d)^3$; (b) top view of (a). The angle between the polarizable axes of adjacent layers is θ .

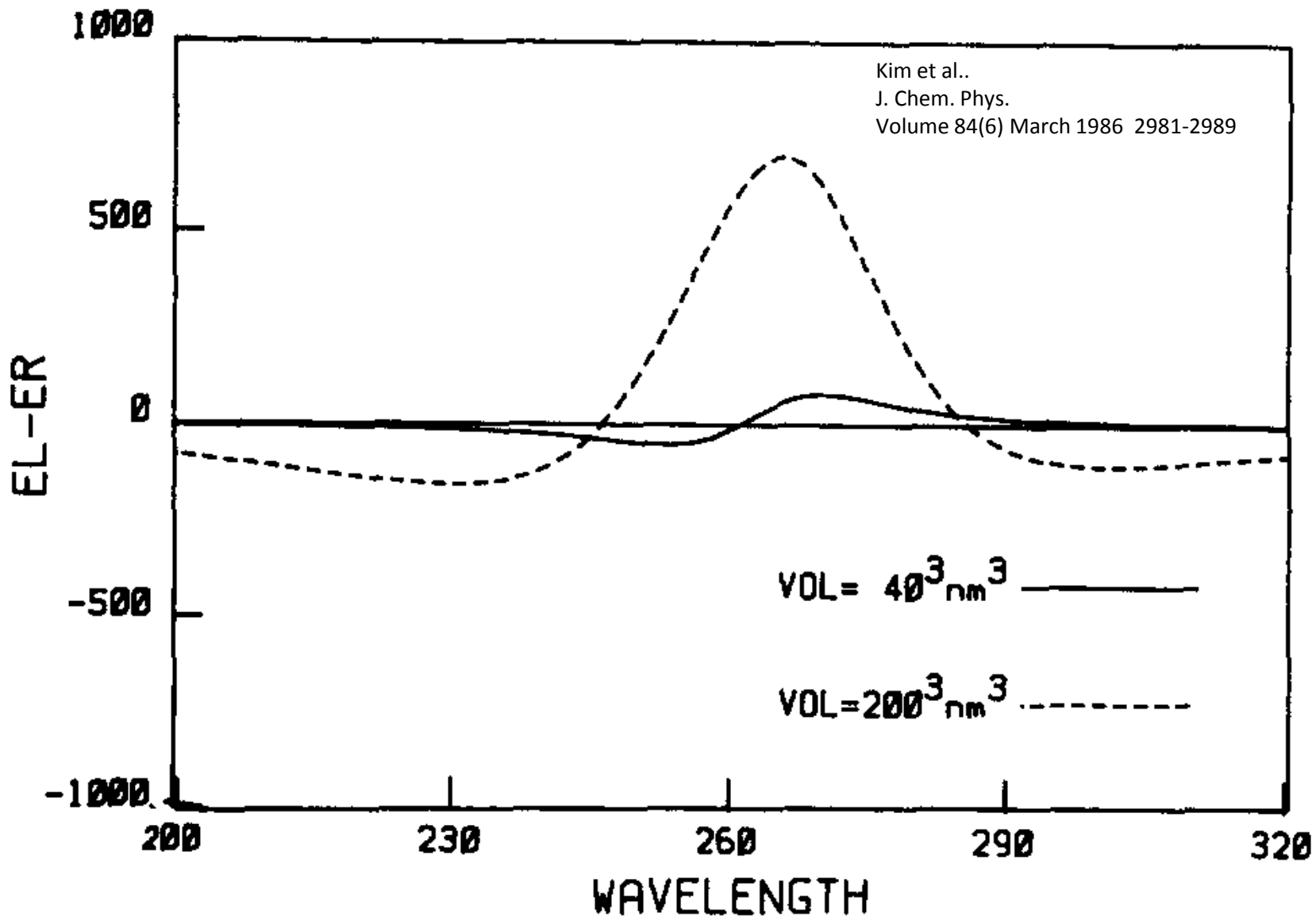
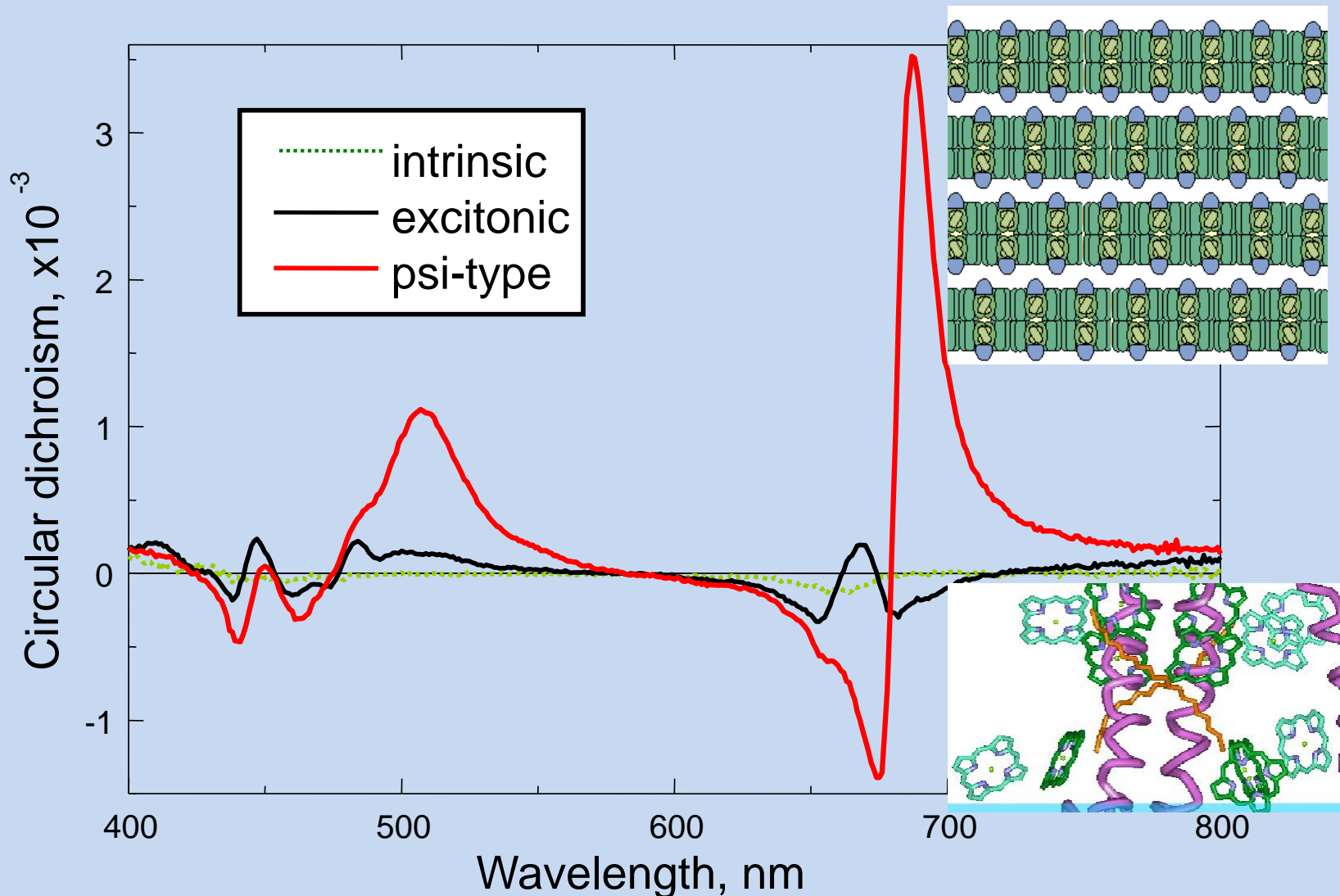
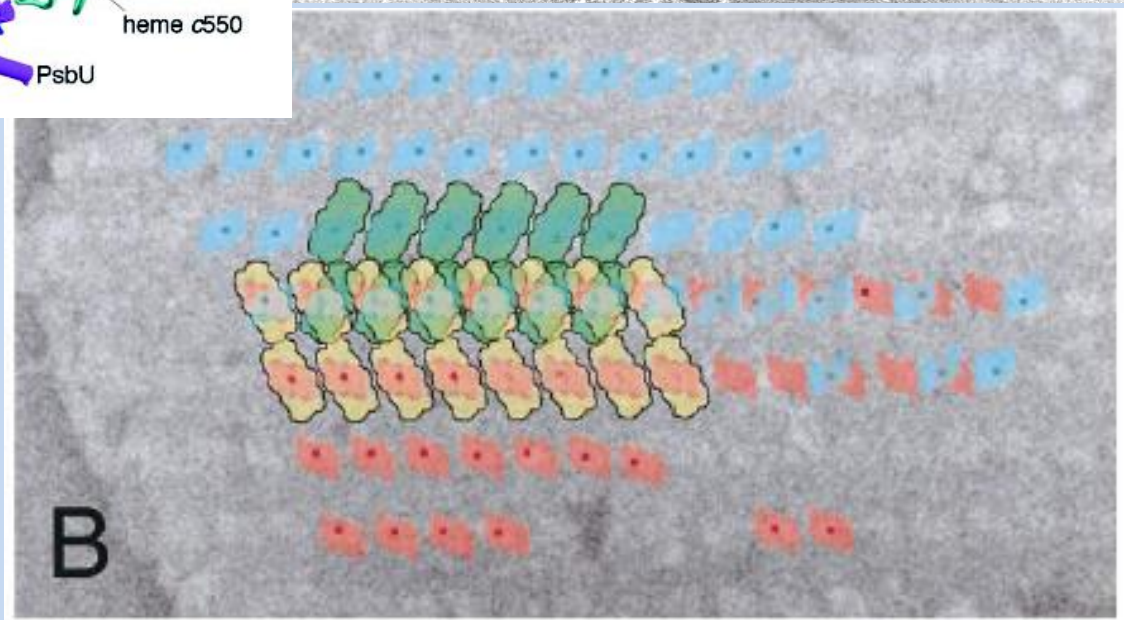
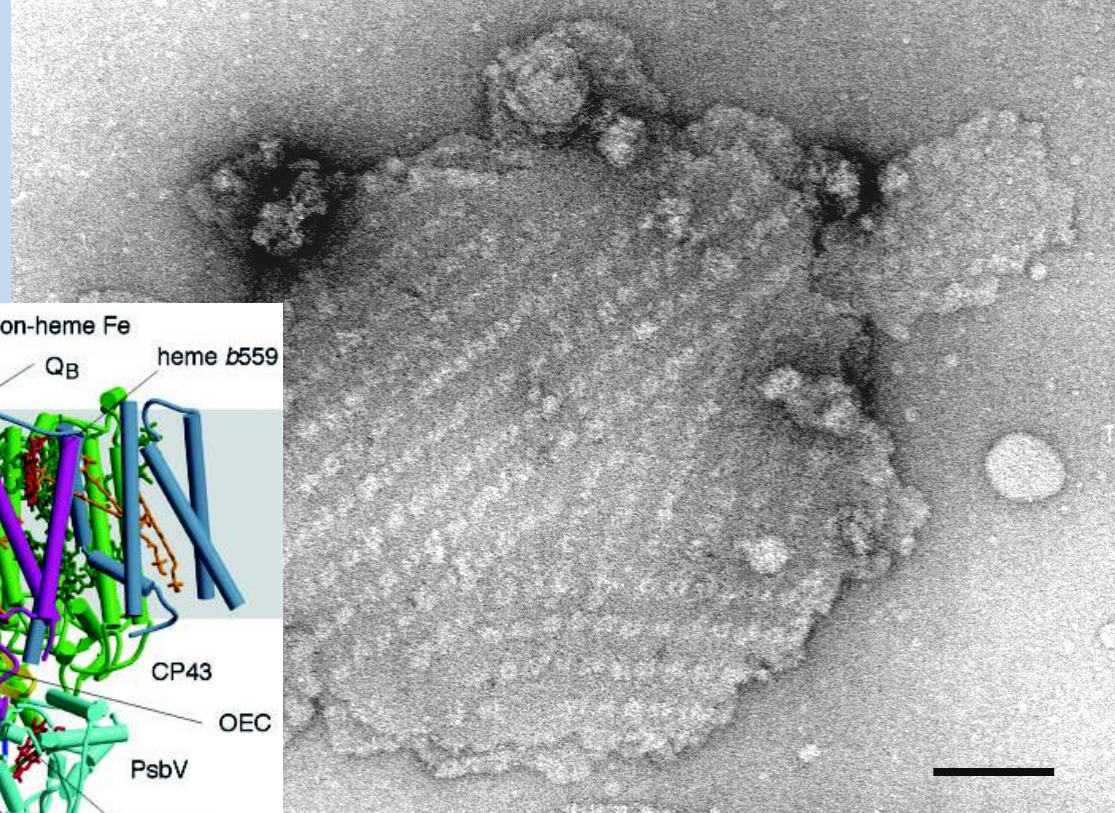
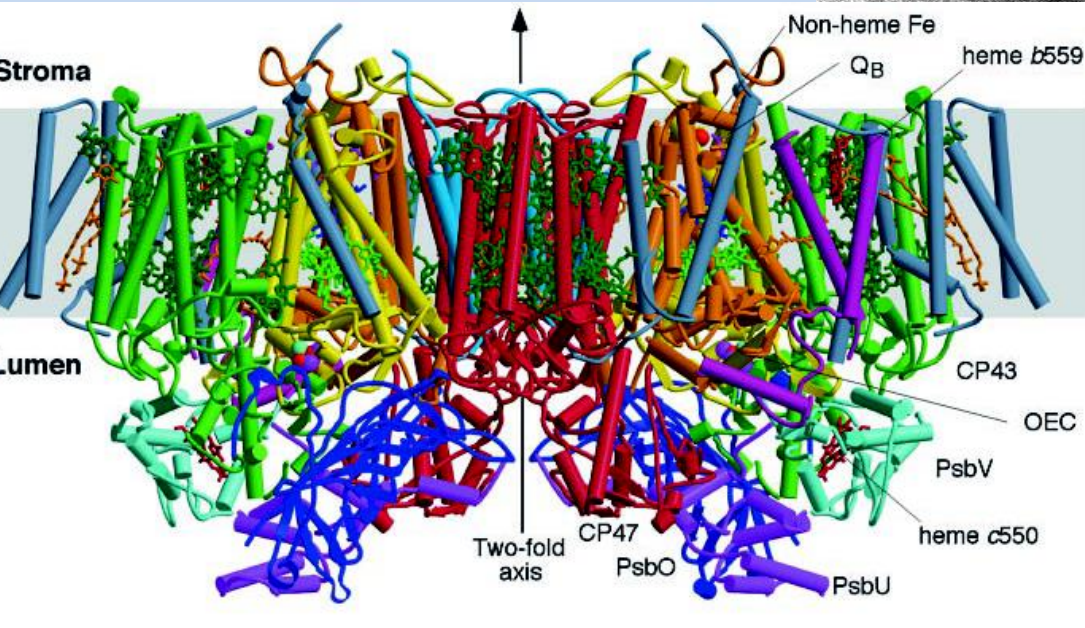


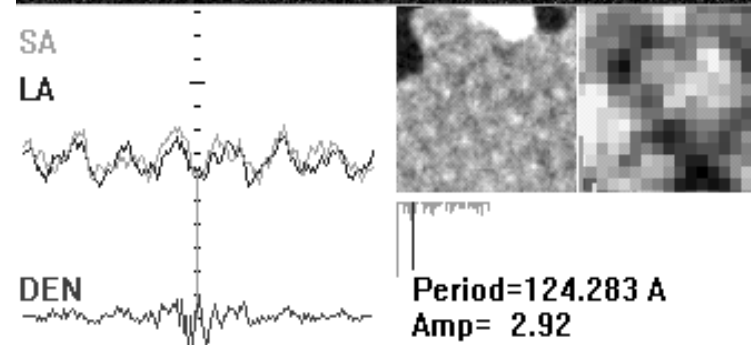
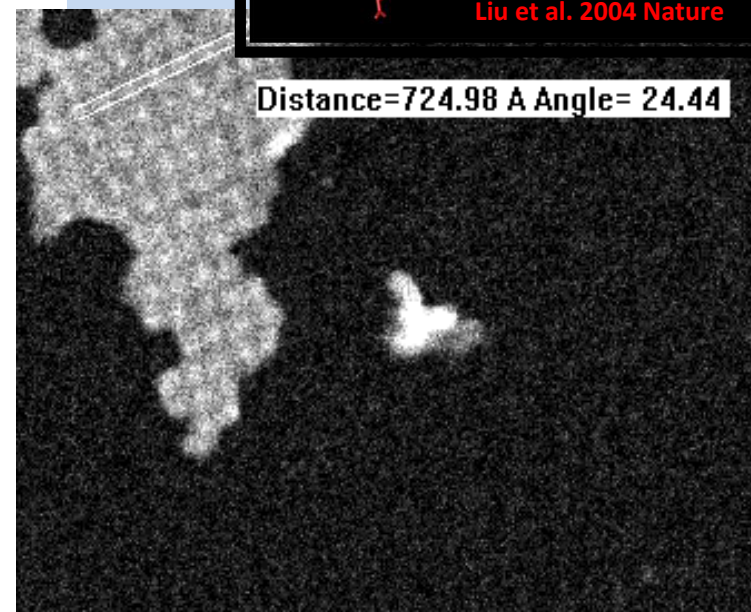
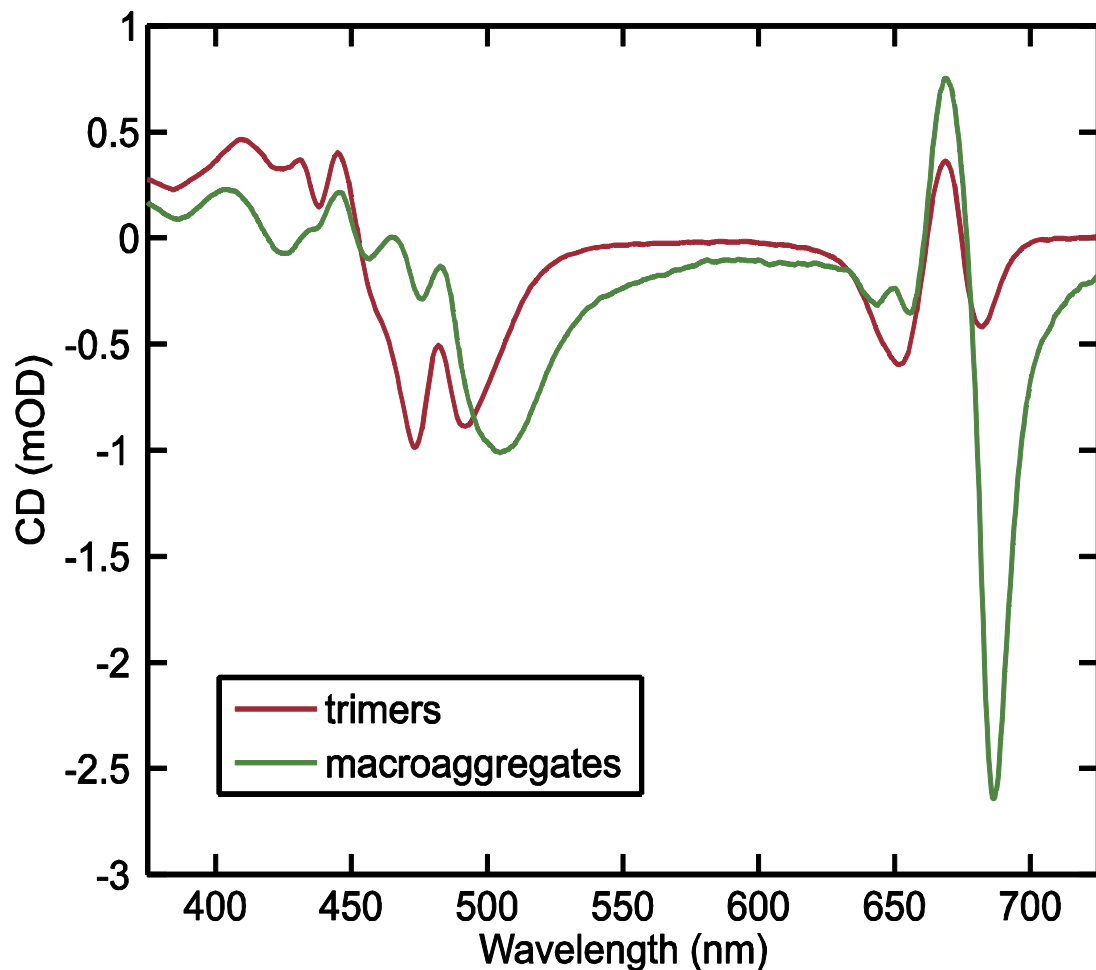
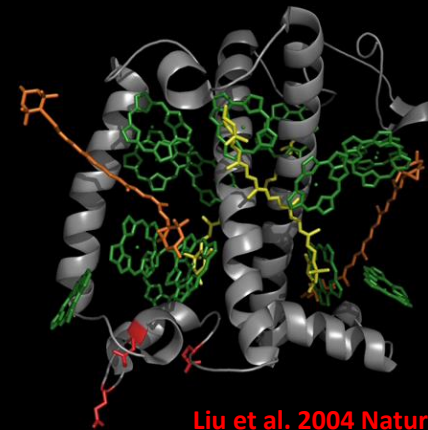
FIGURE 3 The CD spectra of aggregates with different sizes: The pitch and the chromophore density are the same for both aggregates, which are 300 nm and 2 chromophores/ nm^3 , respectively. (1) The solid line: volume = 40^3 nm^3 ; (2) the dashed line: volume = 200^3 nm^3 .

CD spectra of thylakoid membrane pigments at different levels of the structural hierarchy





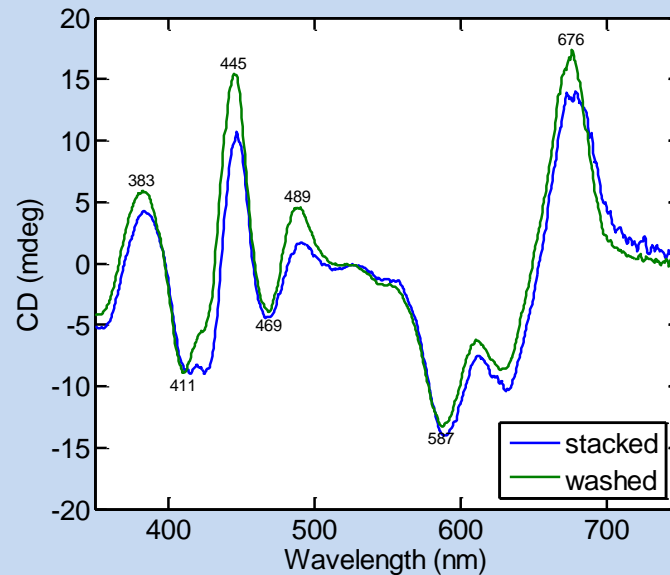
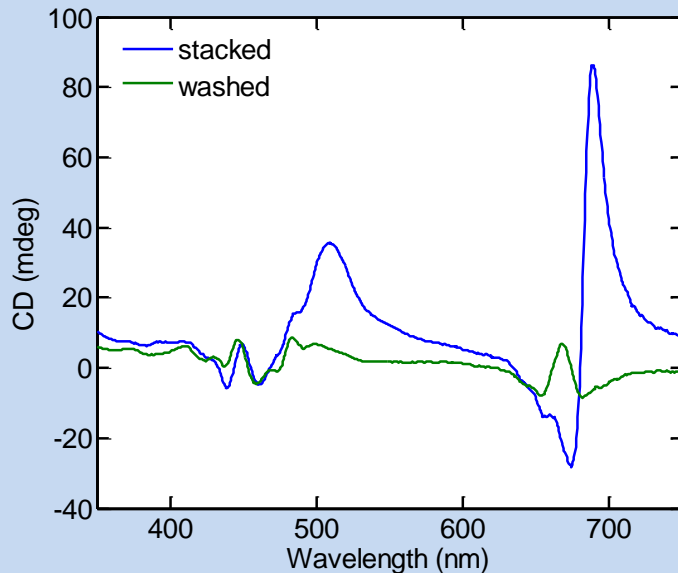
CD of LHCII samples



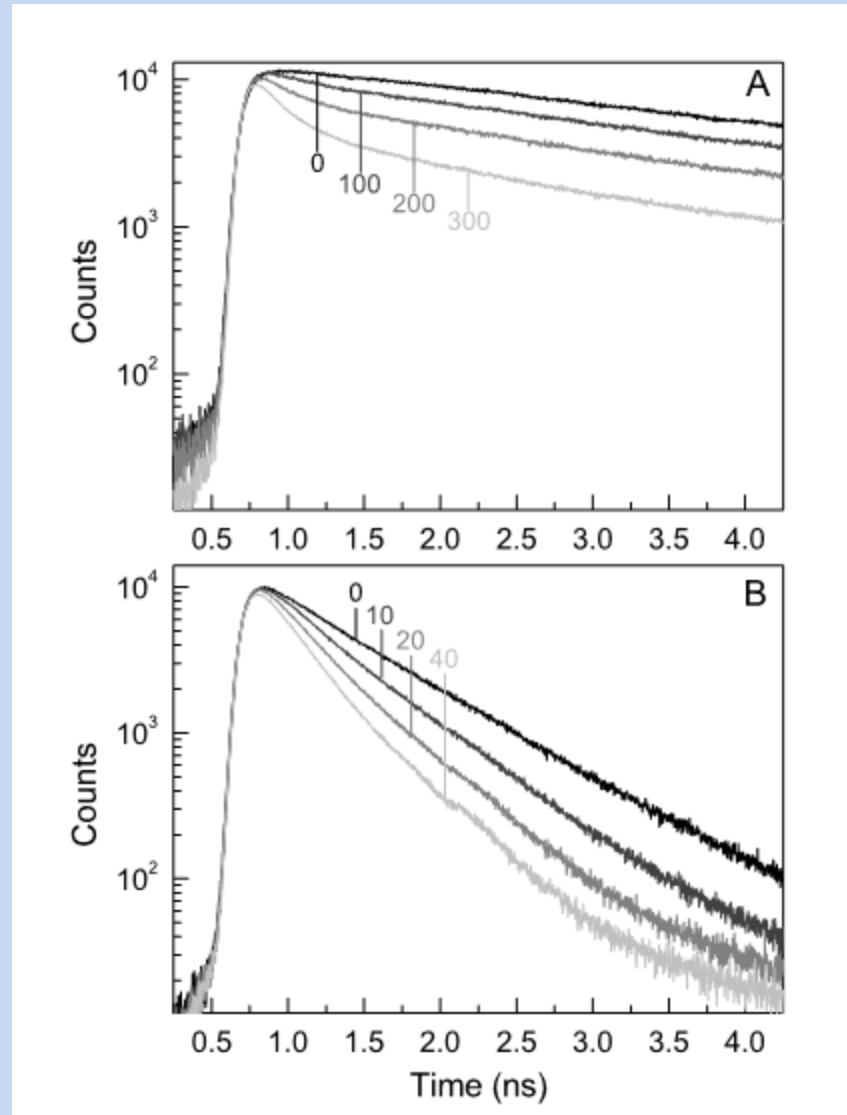
CD and Magnetic CD

- MCD is the CD induced by magnetic field
- MCD is not affected by
 - supramolecular organization
 - orientation of the sample
 - differential scattering

Thus, an an ,internal standard', shows that psi-type CD is not an optical artefact.



The effective (functional) domain size



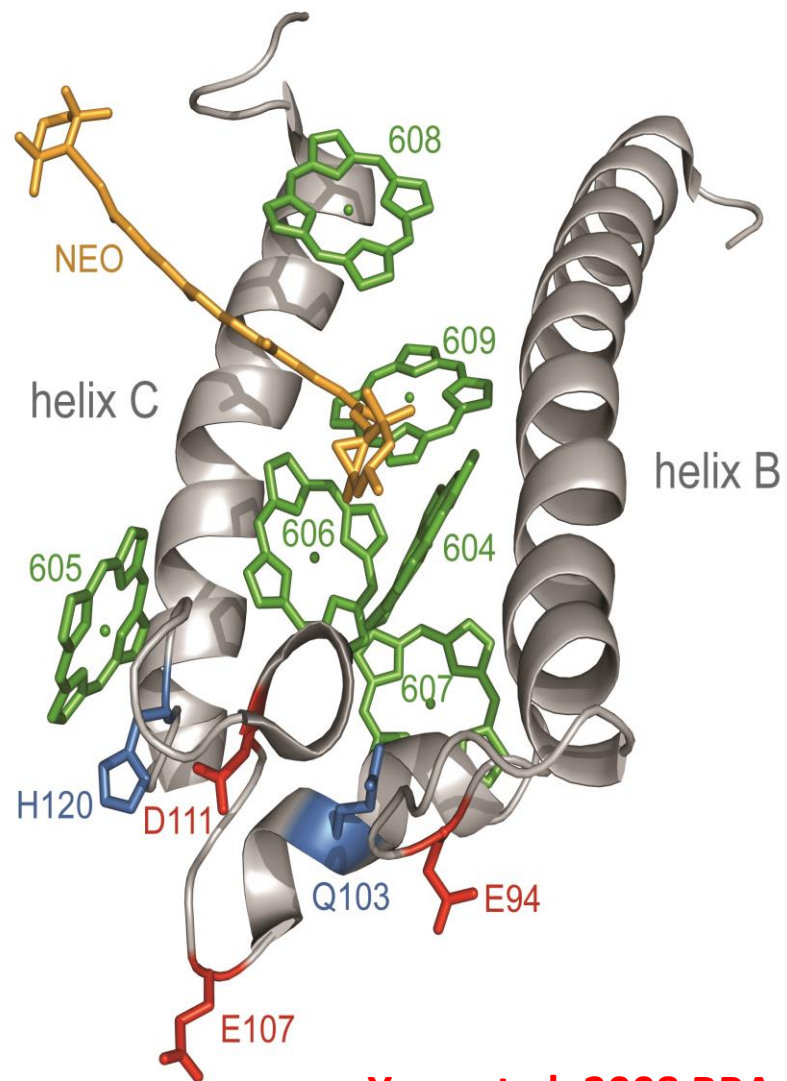
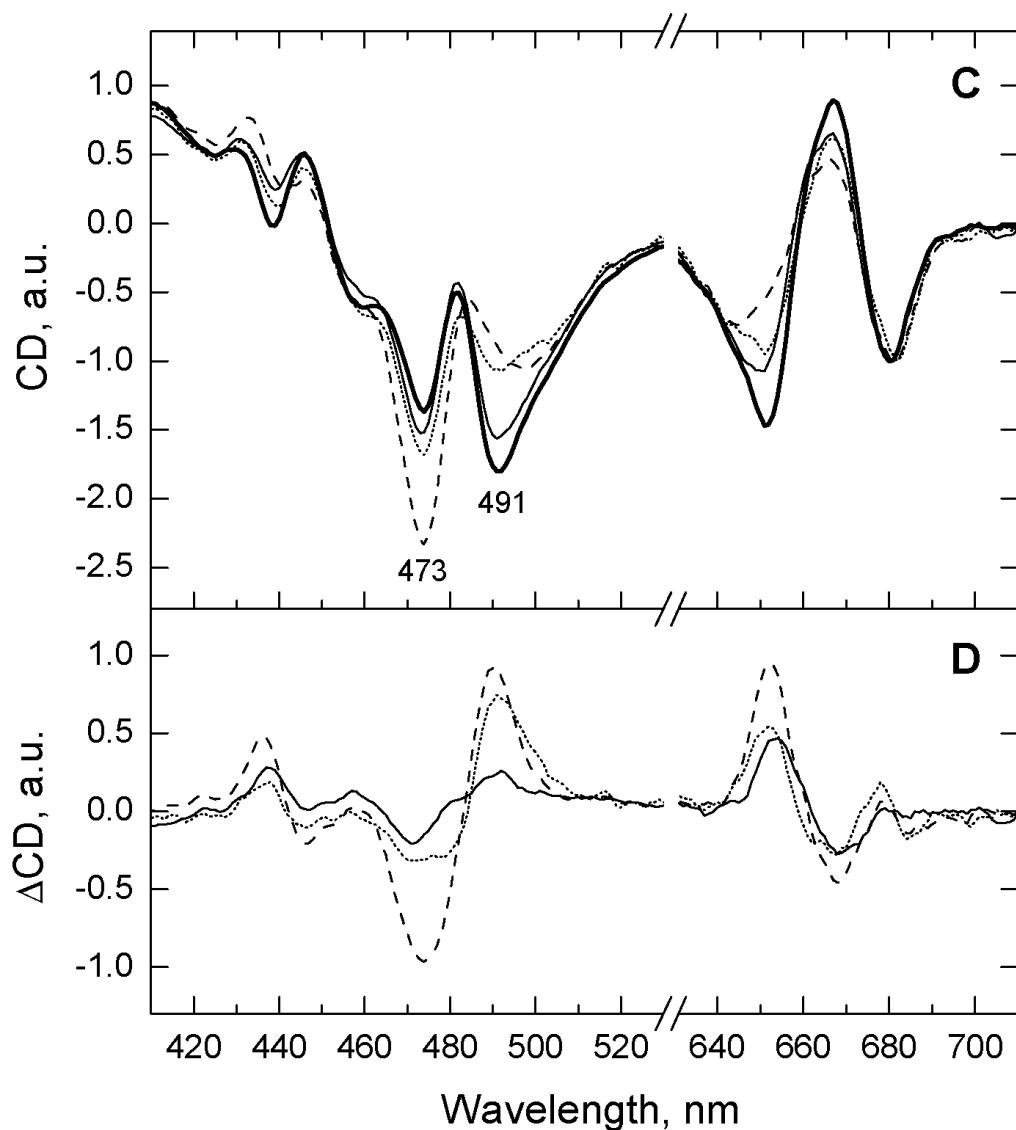
Fluorescence decay kinetics of solubilized LHCII trimers (exc. 632 nm, detected 682 nm)

Fluorescence decay kinetics of LHCII macroaggregates in the presence of different concentrations of PPQ (phenyl-*p*-benzoquinone) (exc. 632 nm, detected 682 nm)

Table 2. Apparent quenching rates K_Q and calculated domain sizes N in isolated LHCII.

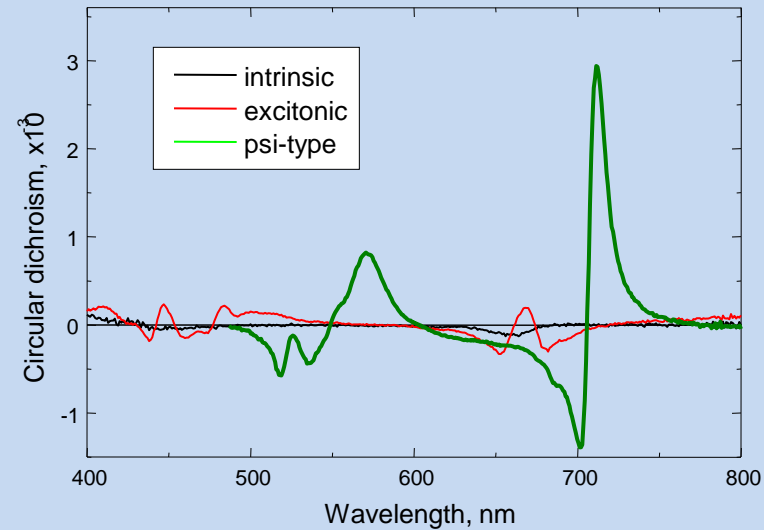
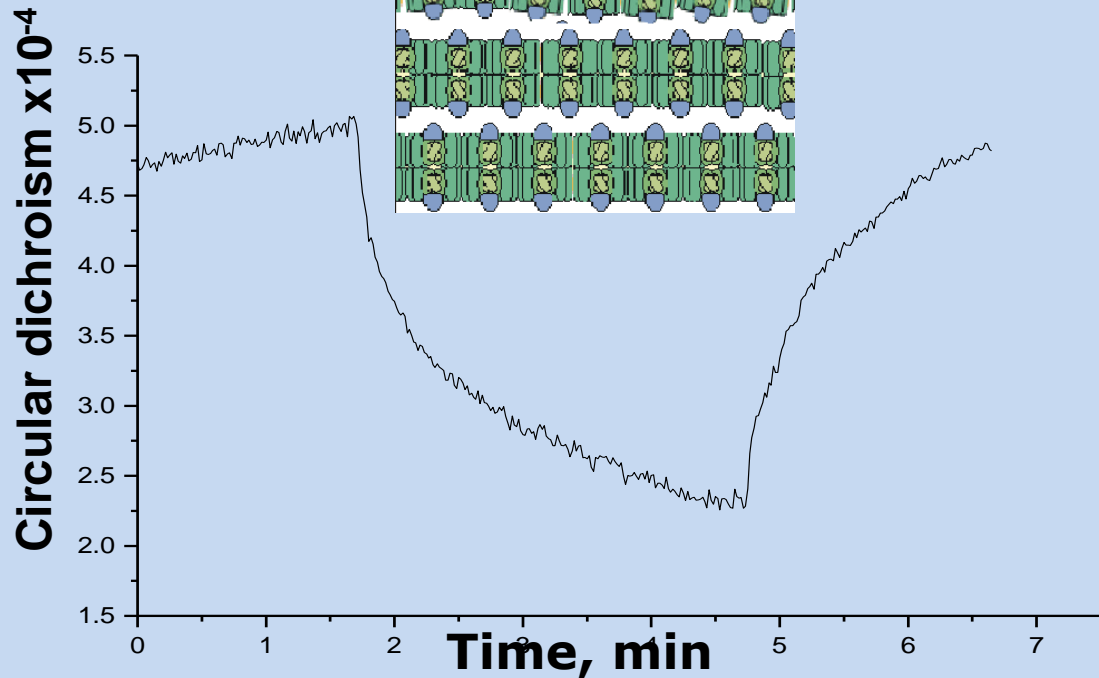
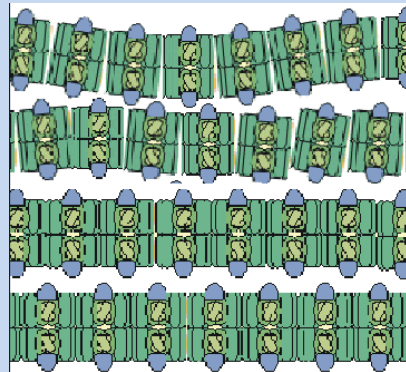
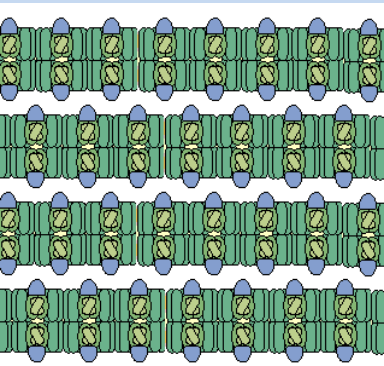
Quencher	LHCII type	K_Q ($M^{-1} ps^{-1}$)	N	Unit
PPQ	Aggregates (Bio-beads)	97.6	30	trimers
	Lamellar macroaggregates	83.0	25	trimers
	Aggregated LHCII monomers	47.9	31	monomers
	Trimers	3.3	3	monomers
	Monomers	1.5		
DNB	Aggregates (Bio-beads)	3.0	15	trimers
	Lamellar macroaggregates	4.9	25	trimers
	Trimers	0.2		

Sensitivity of excitonic interactions to minor changes in the protein scaffold

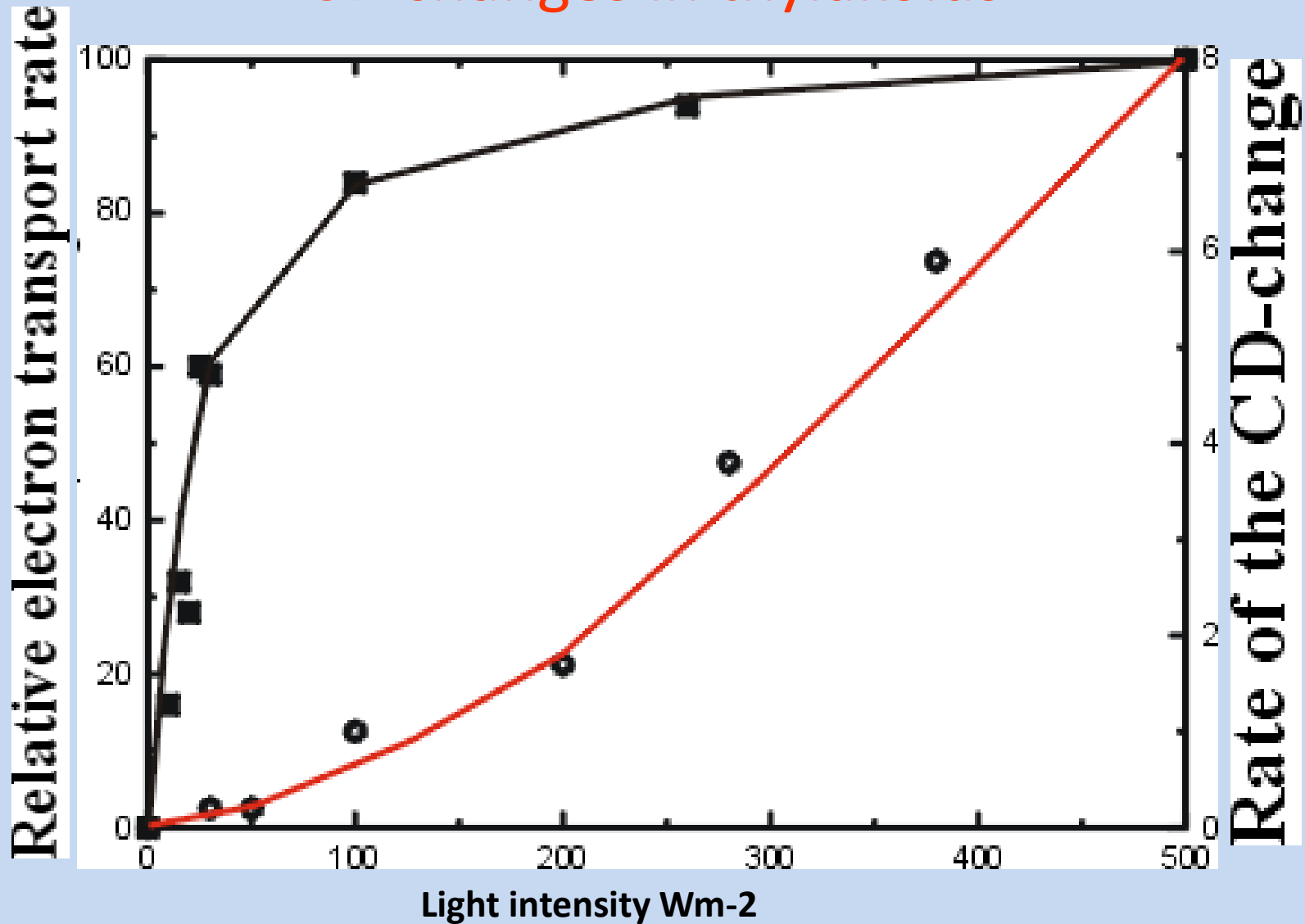


Yang et al. 2008 BBA

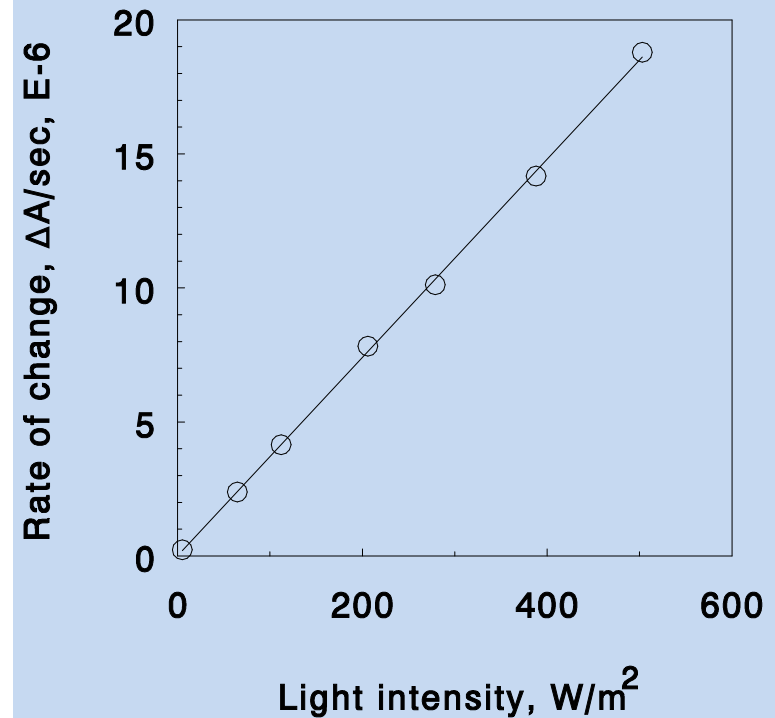
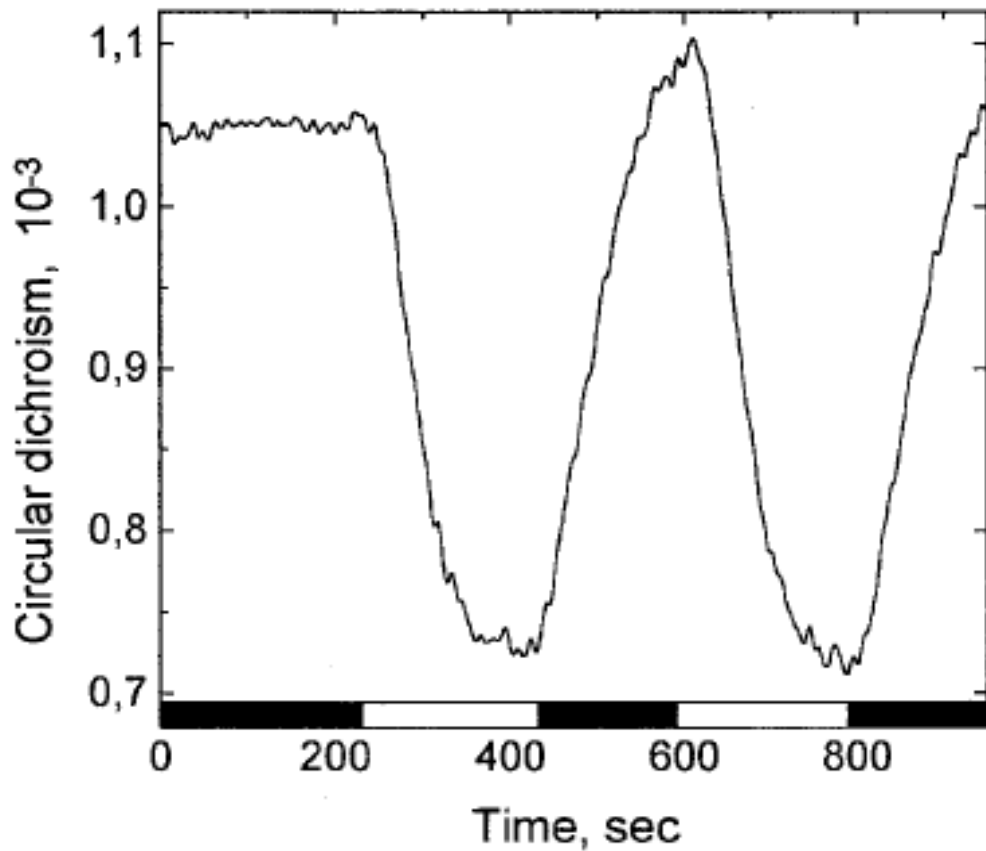
Light-induced reversible reorganizations in the chiral macrodomains of thylakoid membranes



Quasi-linear light intensity dependence of the CD changes in thylakoids

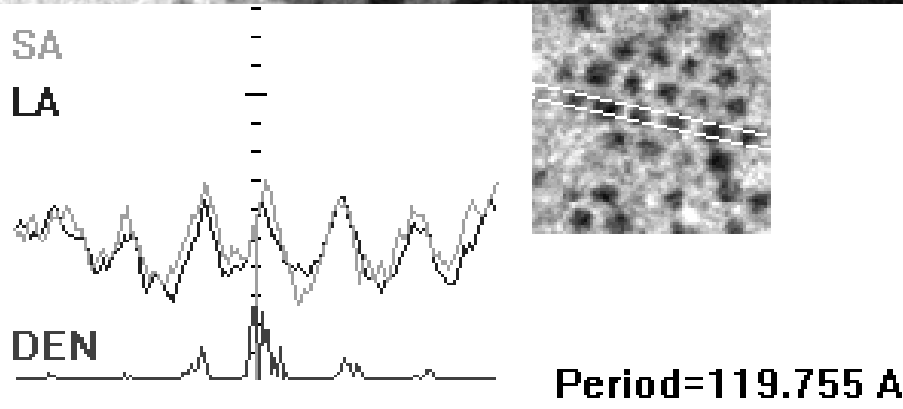
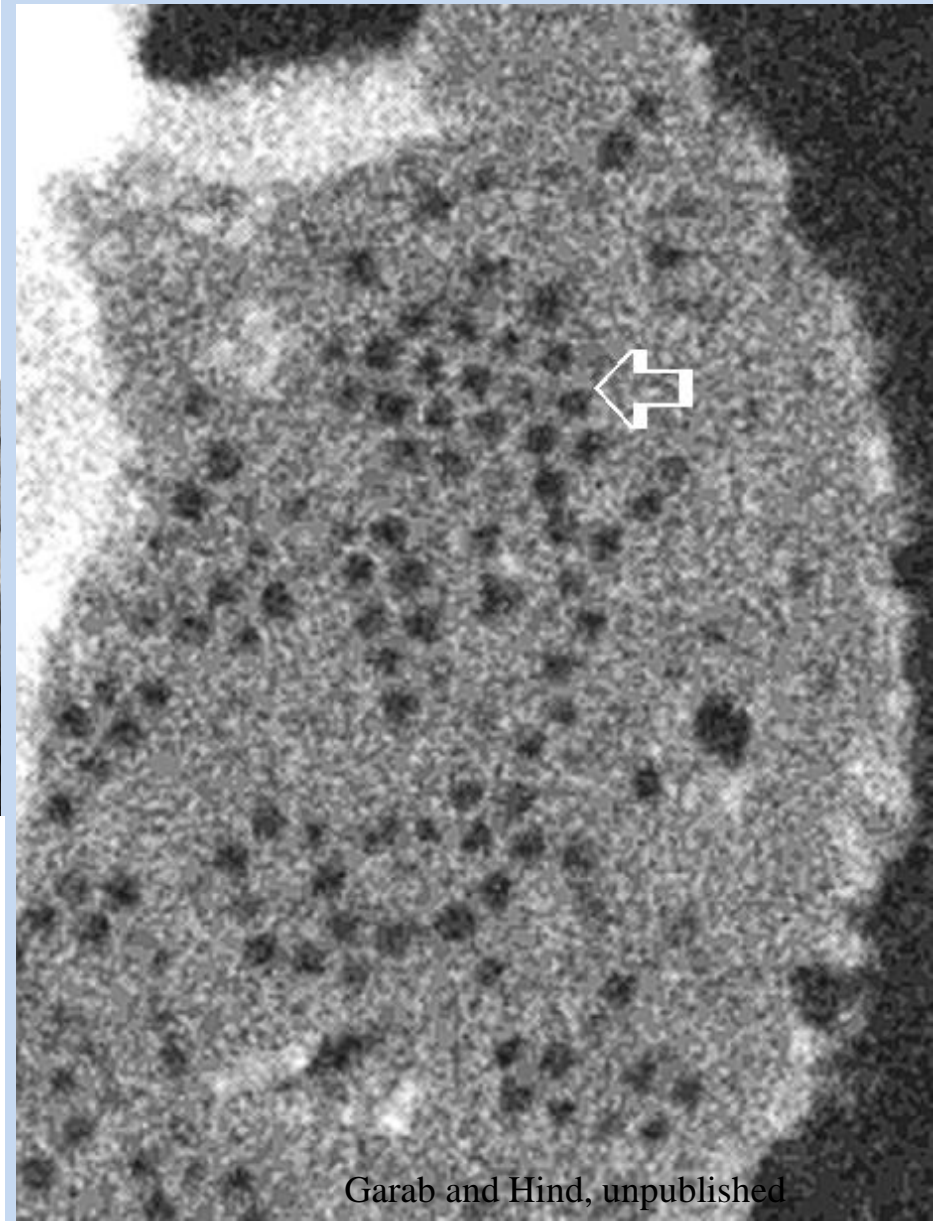
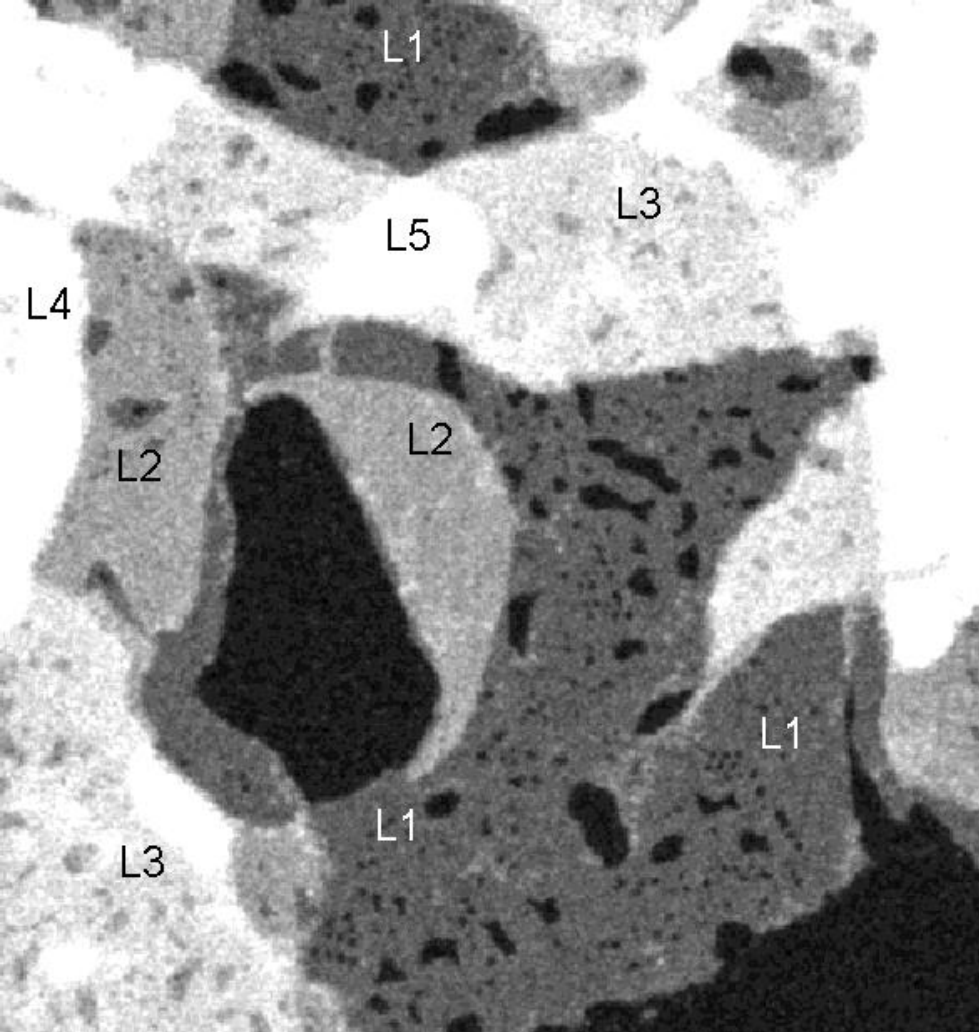


Thermo-optically induced reversible reorganizations in lamellar aggregates of LHCII

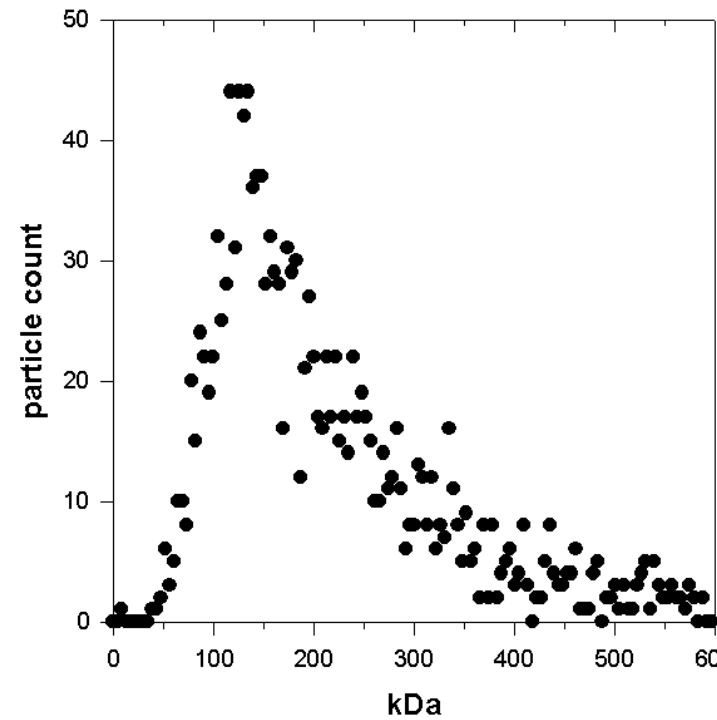
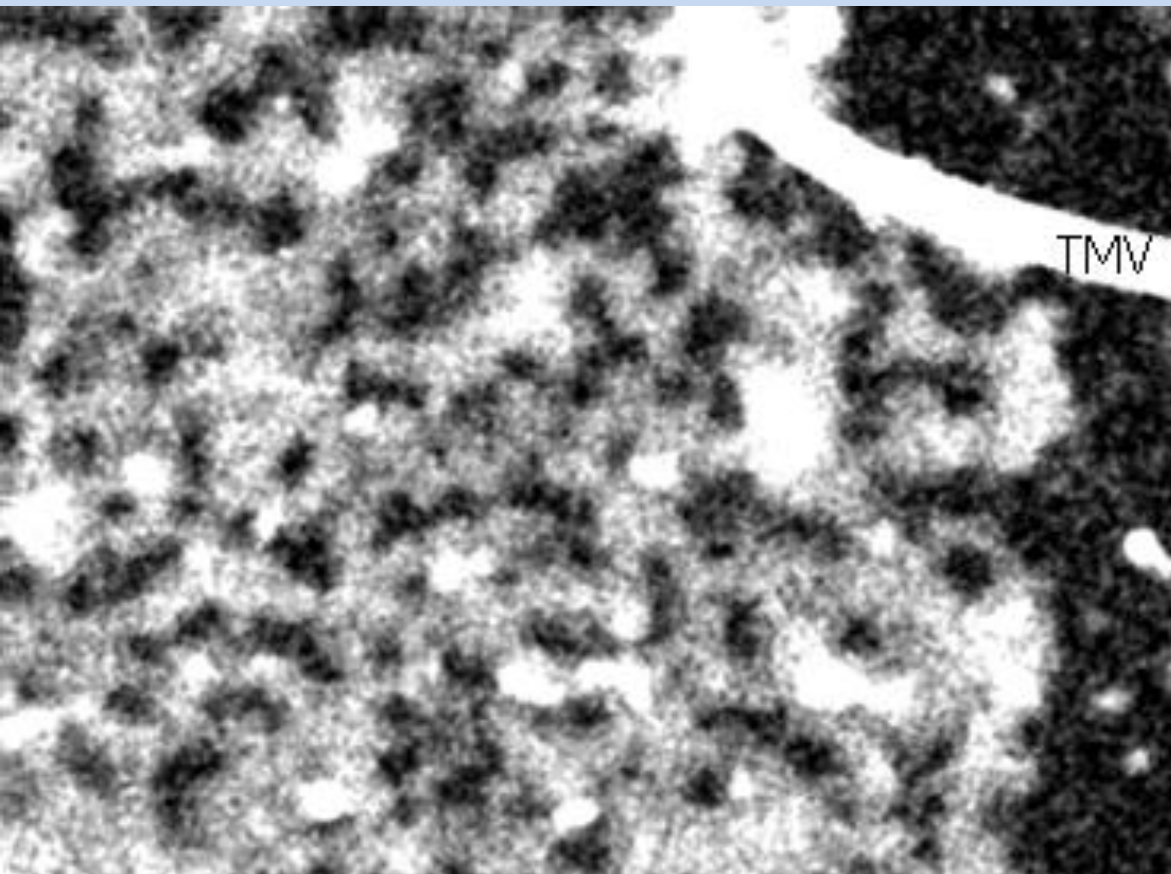


Simidjiev et al. Anal Biochem 1997, Cseh et al. 2005 Photosynth. Res.

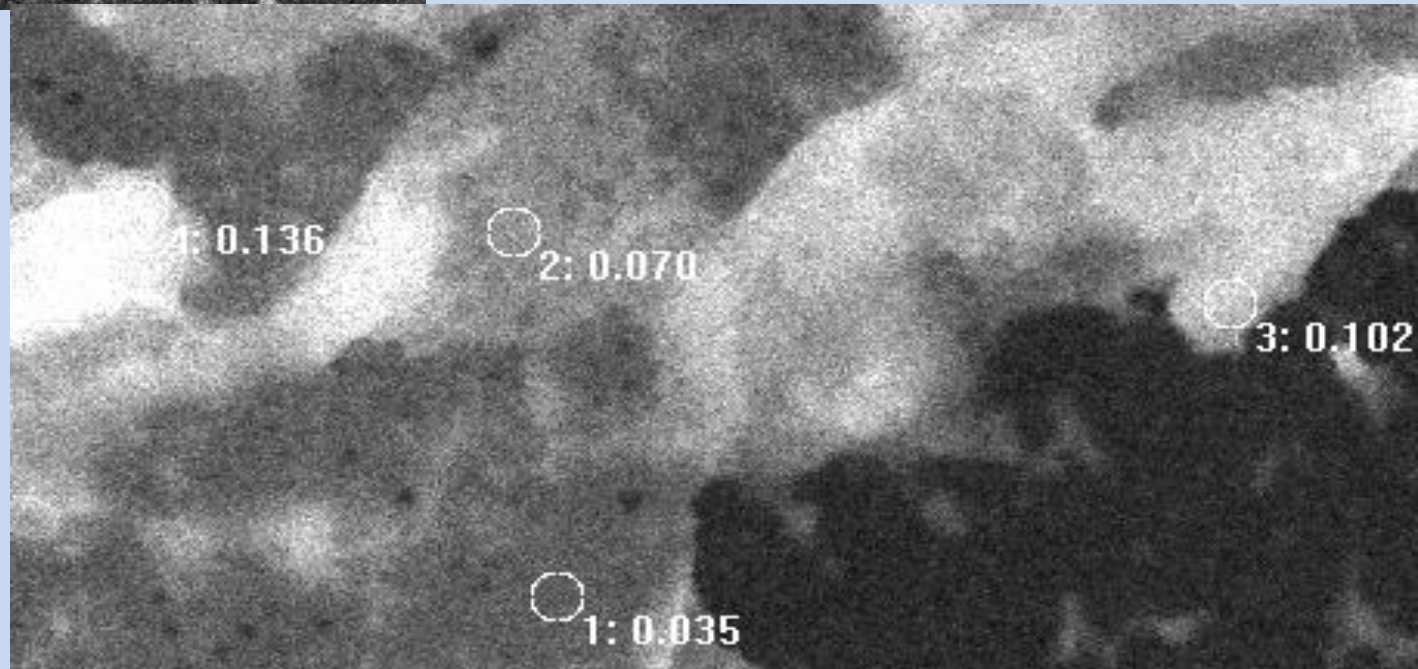
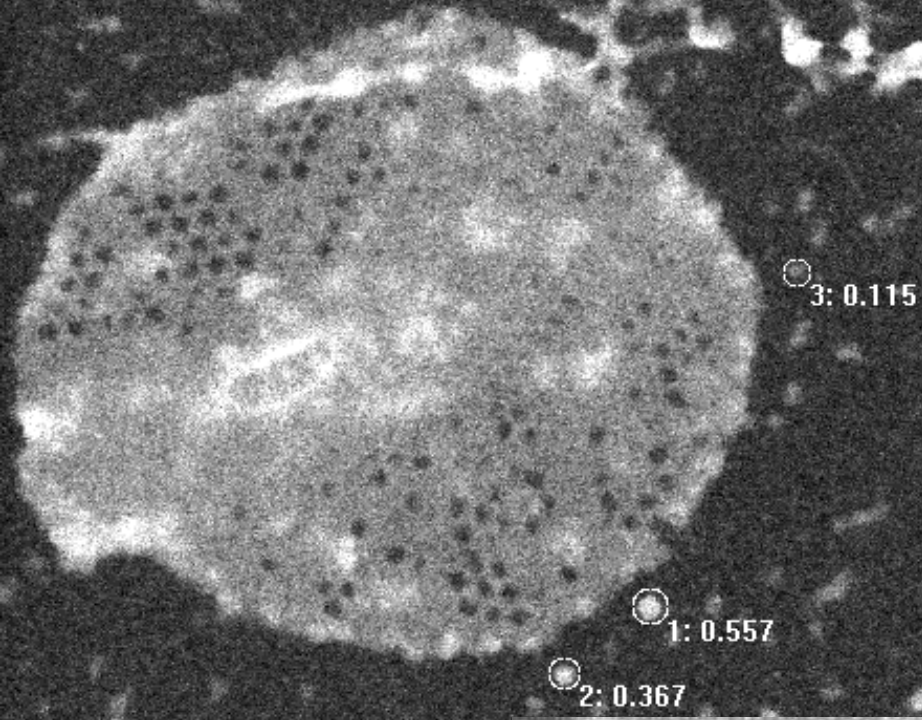
STEM of LHCII in the dark



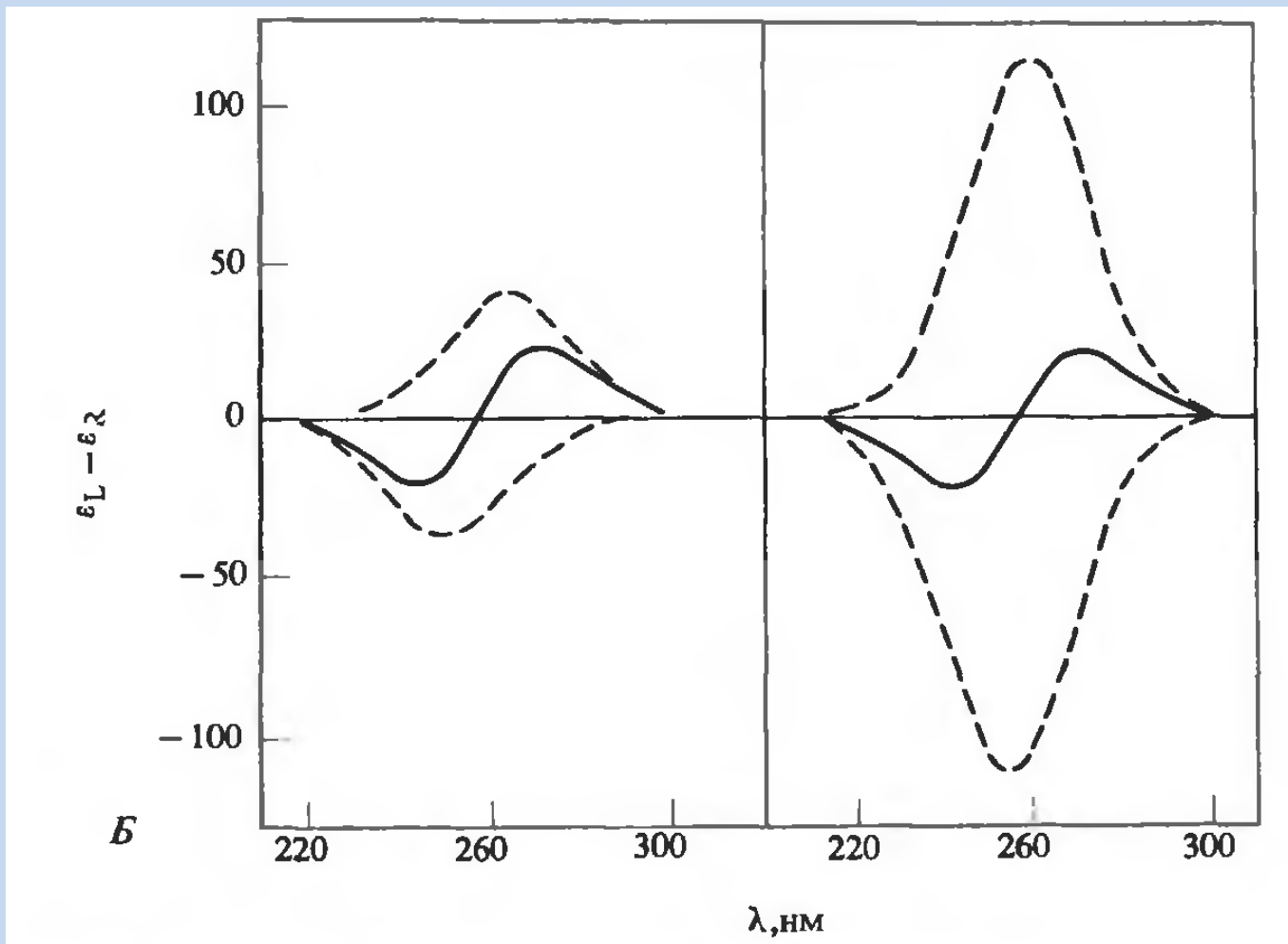
STEM of LHCII after preillumination (3 min 2000 μE)



**STEM of LHCII
in the re-dark
(10 min after
preillumination)**



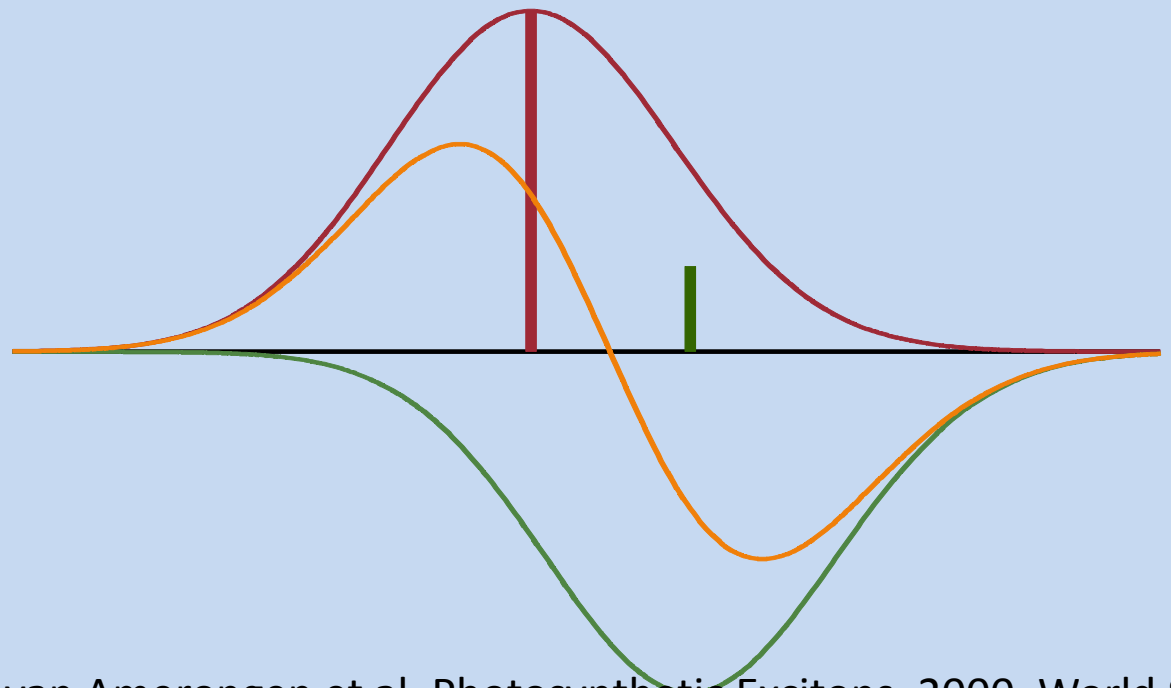
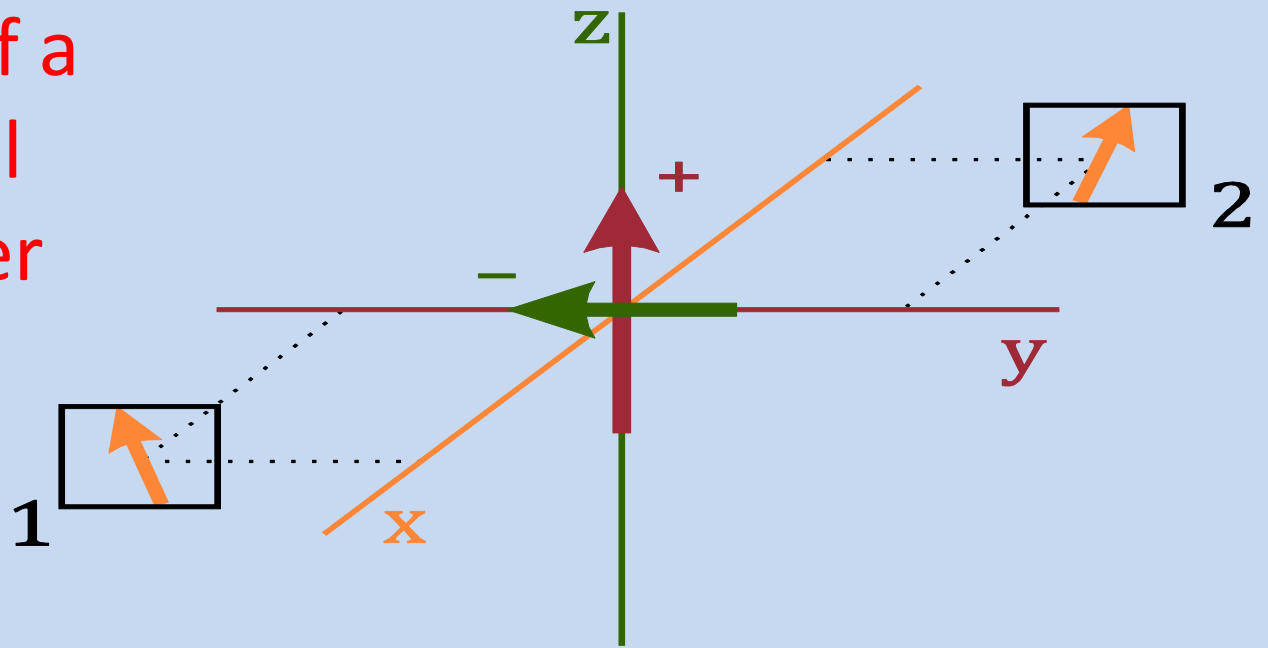
**CD is a sensitive probe of
the (dynamic) molecular
architecture of complexes,
and of their macroarrays**



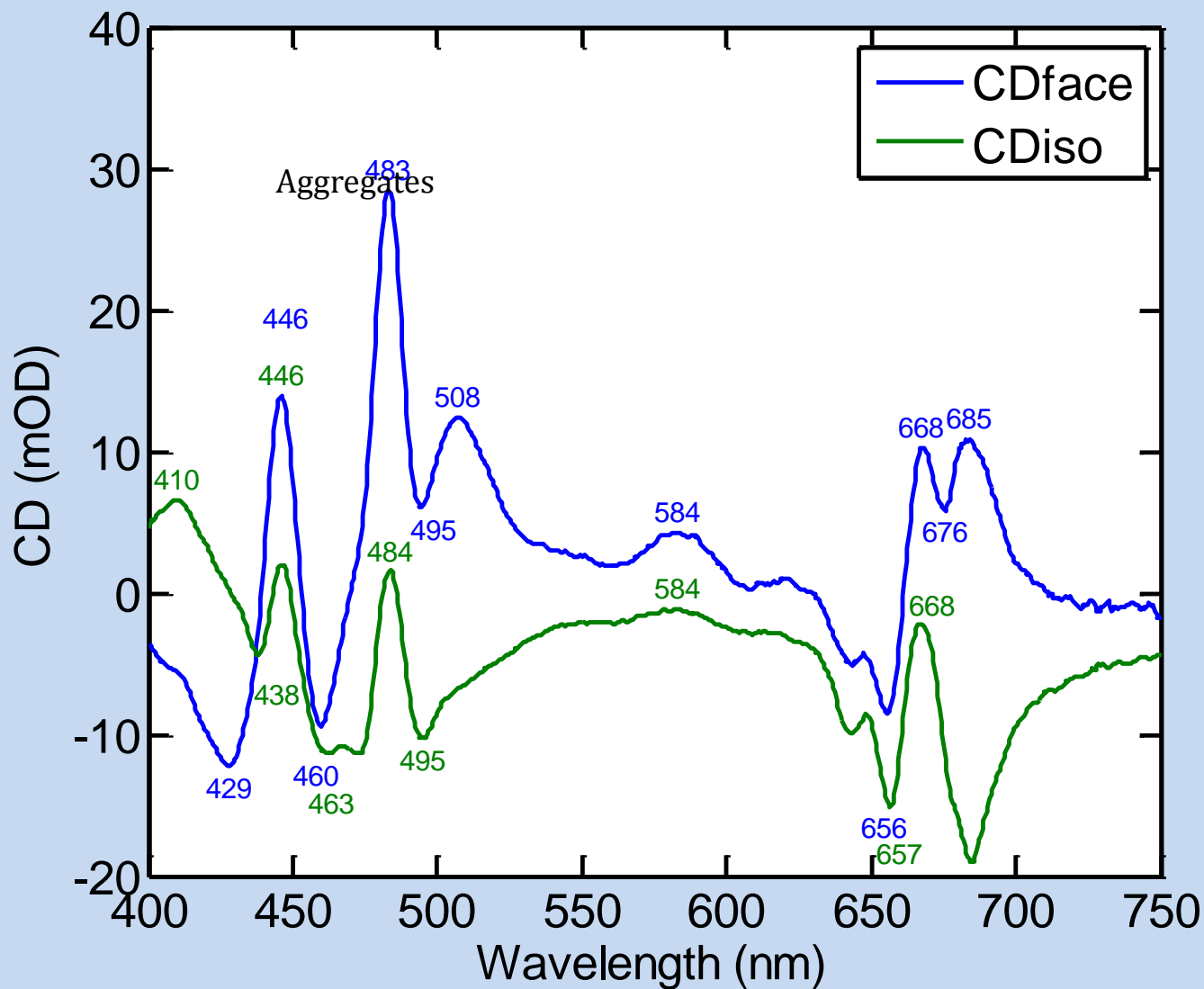
CD of excitonic dimers. Solid line – sum (isotropic) CD. Dashed lines – individual excitonic components. Left – monomers at 15°. Right – monomers at 75°.

Cantor, C.R. & Schimmel 1980 Freeman & Co.

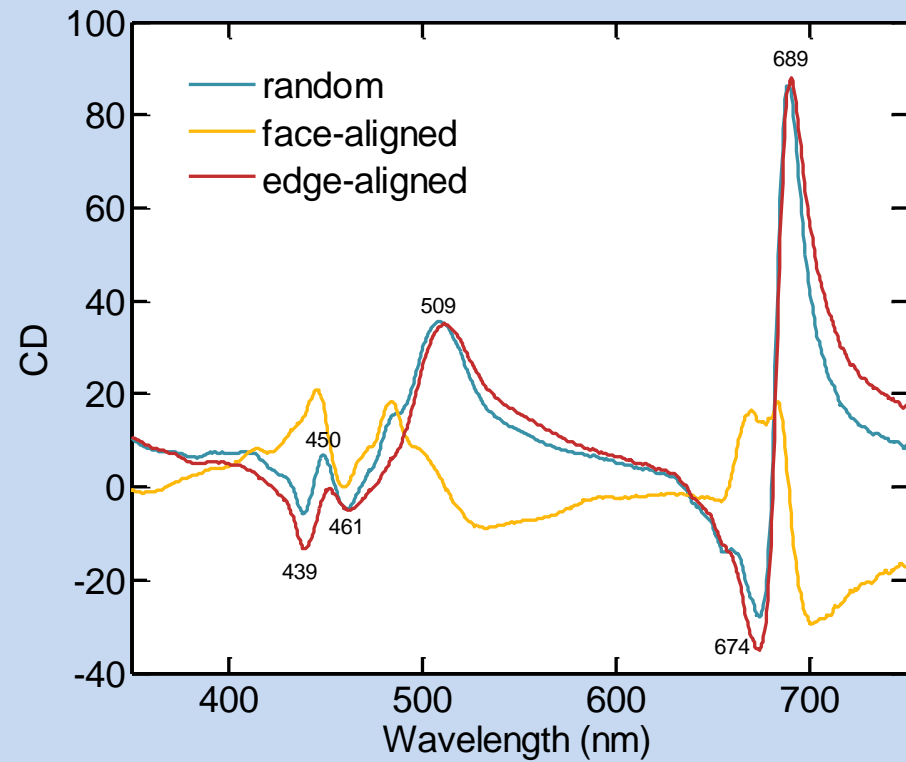
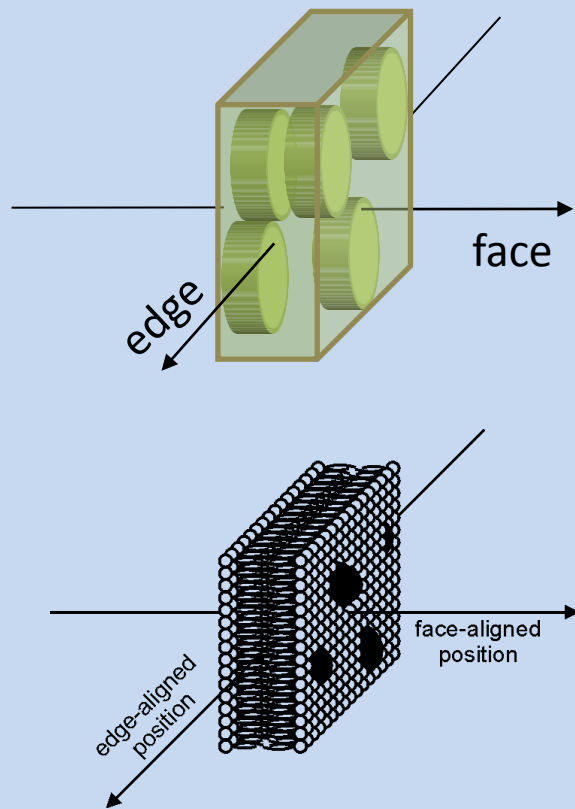
Abs and CD of a hypothetical exciton dimer



CD and ACD of LHClI aggregates

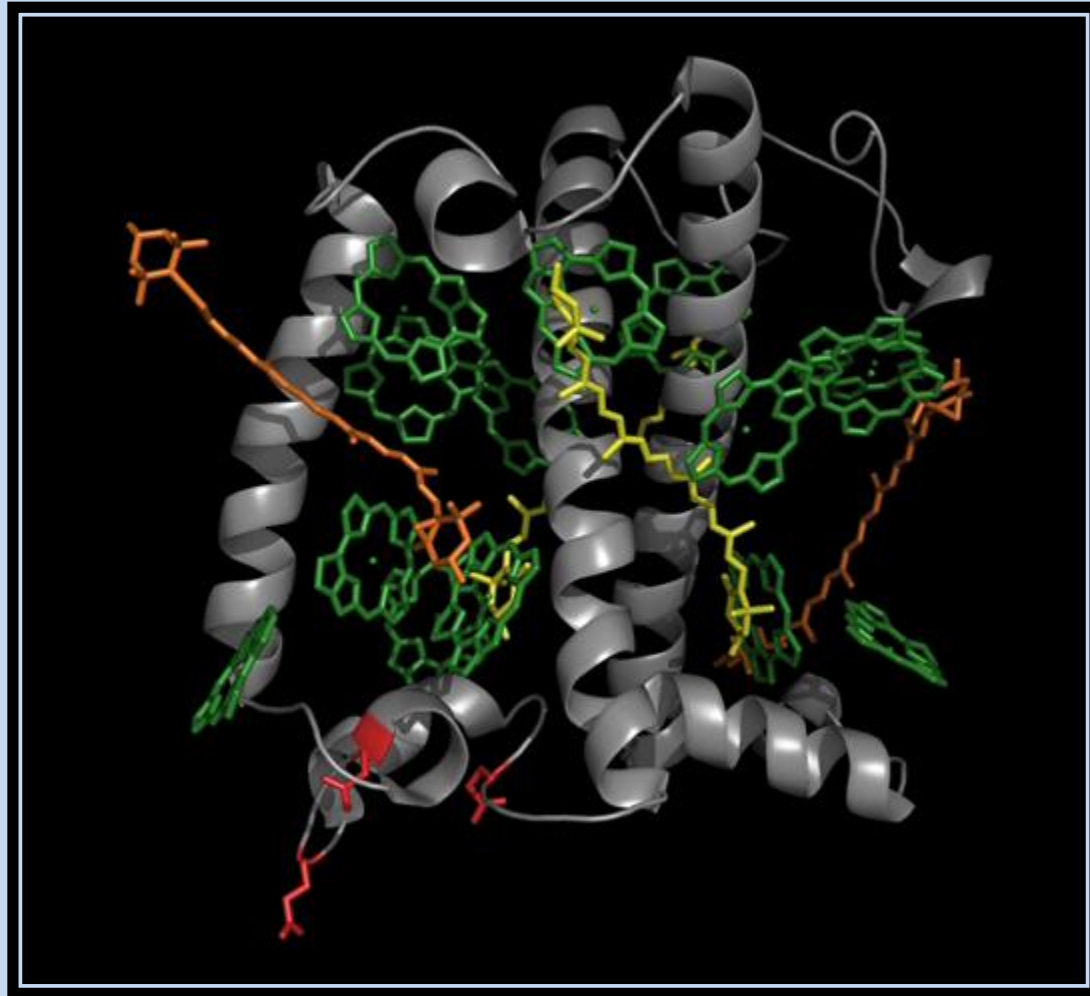


ACD of chloroplast membranes

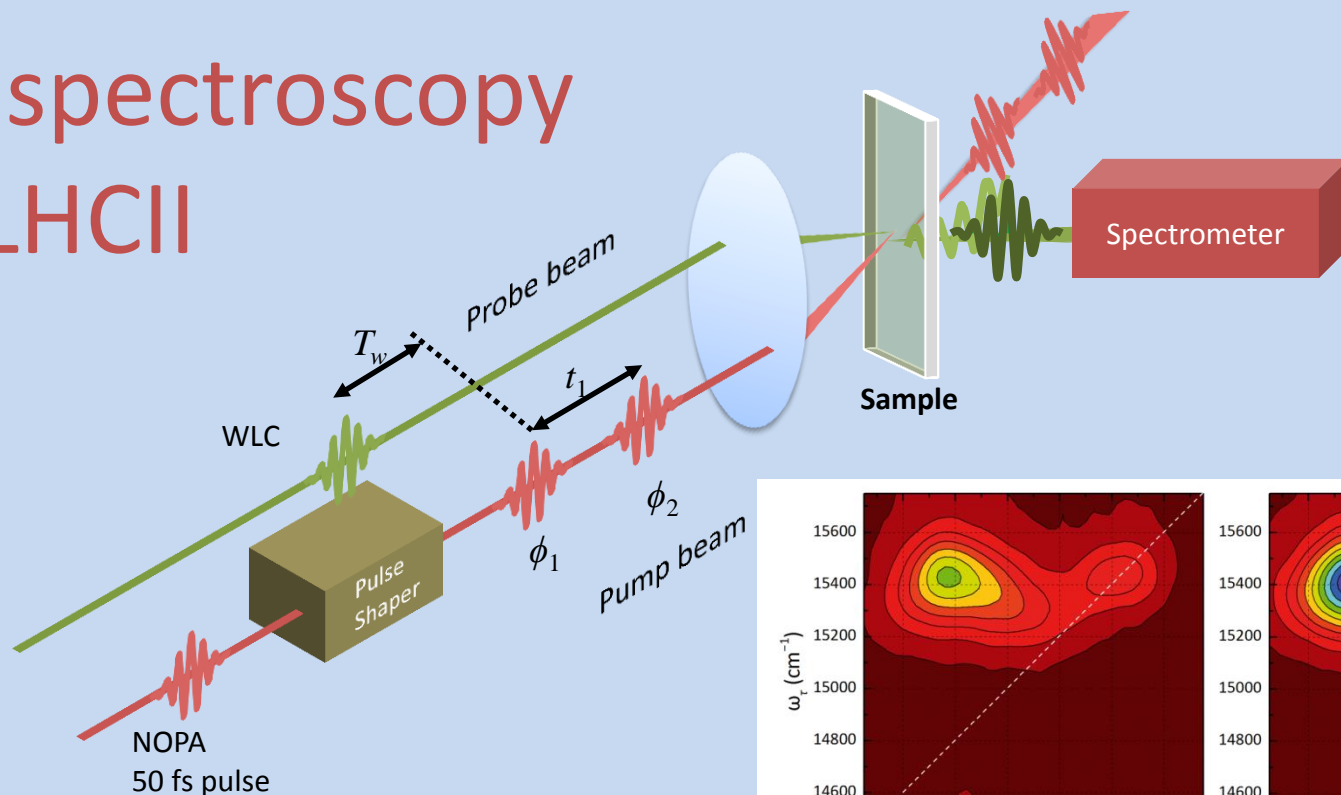


ACD is a (novel) tool to reveal the origin of excitonic interactions in photosynthetic organisms

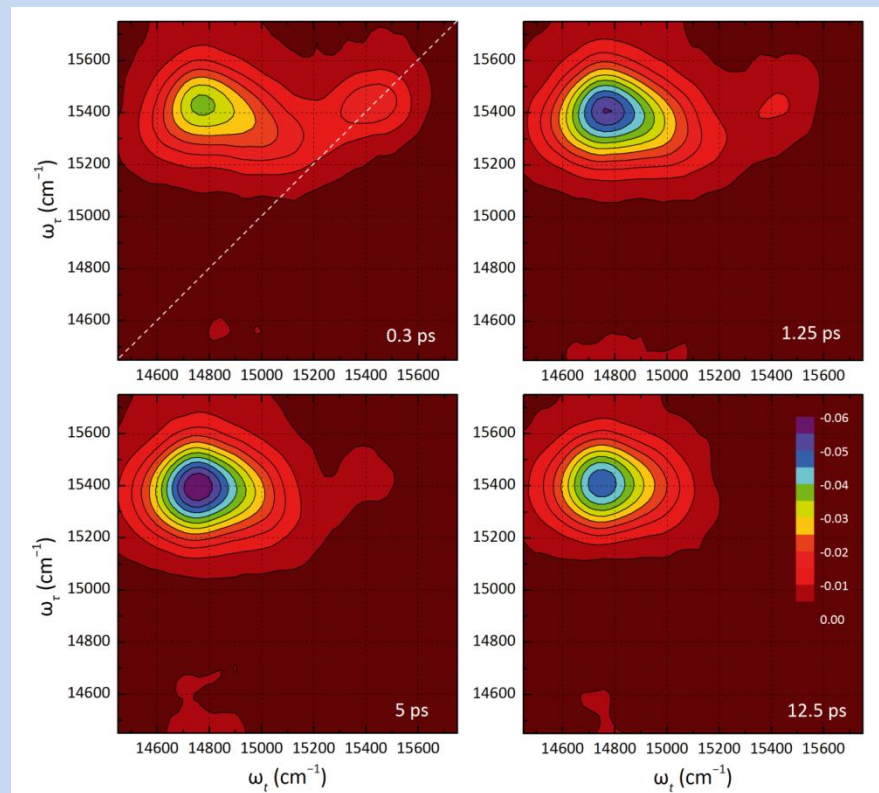
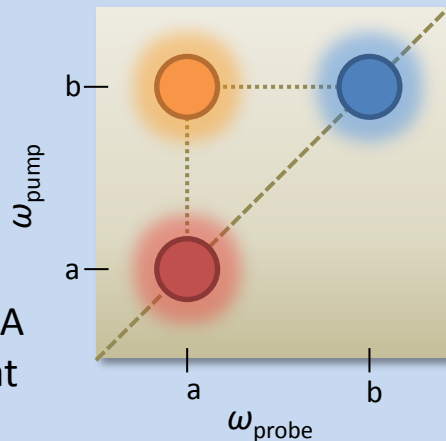
Light-Harvesting Complex II



2D spectroscopy of LHCII



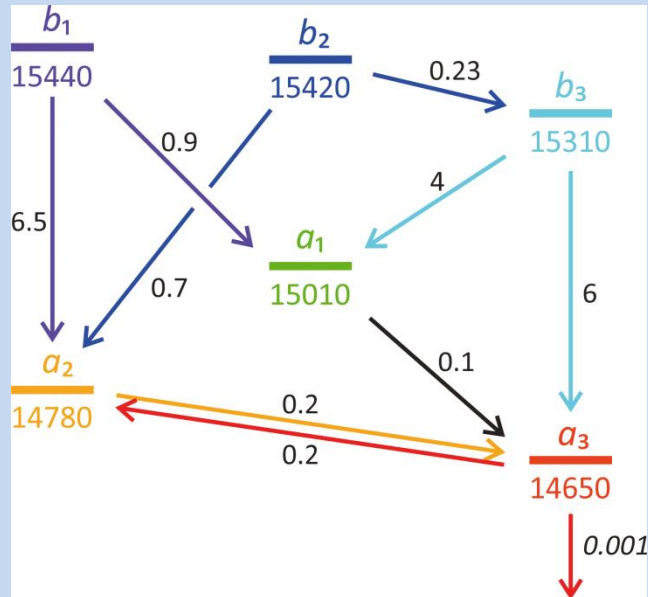
- Two frequency axes in 2D spectra:
 - ‘pump’ frequency reveals initially excited states
 - ‘probe’ frequency reveals coupled transitions
- Energy transfer from B to A manifested as a 2D peak at $\omega_{\text{pump}} = b, \omega_{\text{probe}} = a$



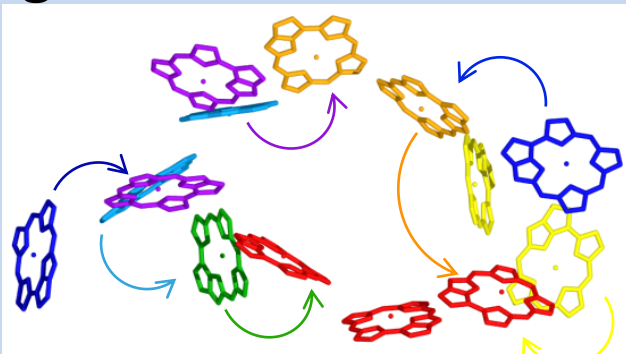
2D spectra of LHCII measured at different waiting times after Chl *b* excitation

Modelling of the 2DES data

Model scheme

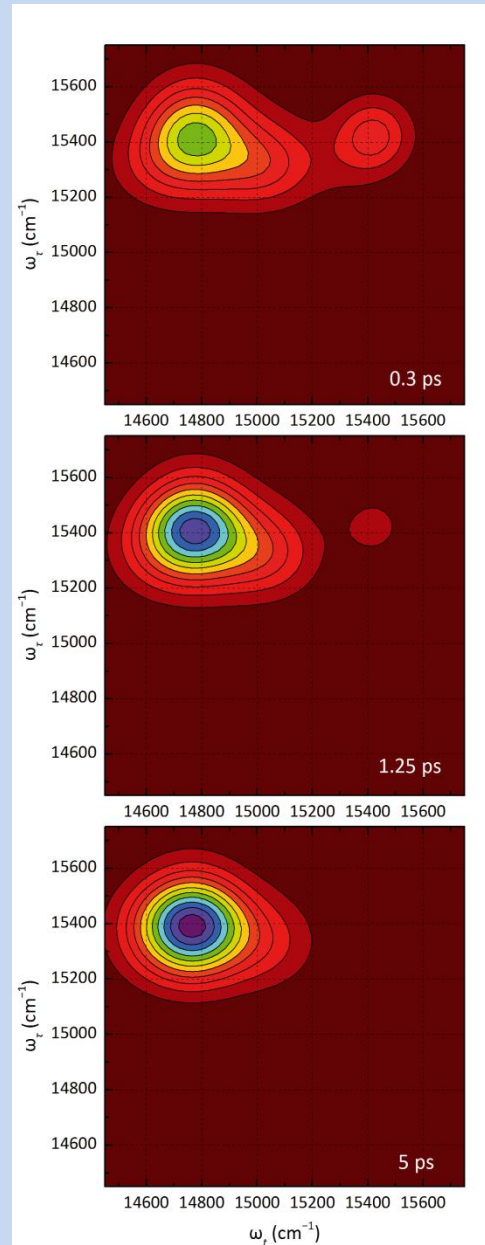


Pigment clusters in LHCII



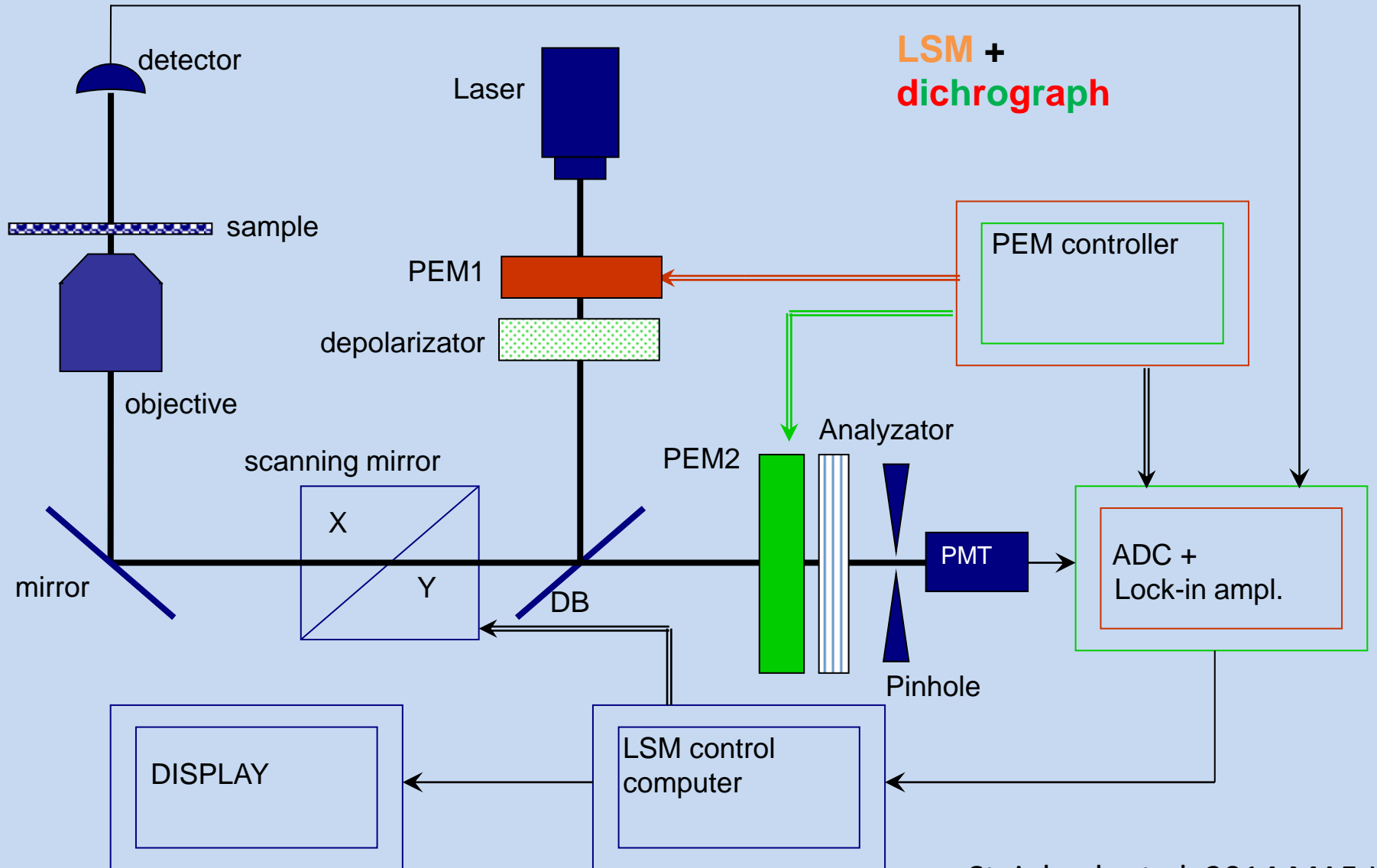
Simulated spectra

- The time-dependent 2D spectra are fitted with a spectro-temporal model
- The modelling results reveal exciton state energies and rate constants of energy transfer
- Simulated 2D spectra reproduce very well the measured ones at all T_w
- Exciton states can be assigned to actual pigments in the structure
- The first experimentally derived model detailed enough to disentangle the complex energy pathways in LHCII (between chl-b and chl-a)



2D spectroscopy is an efficient tool to map the energy migration pathways

General Scheme of DP-LSM





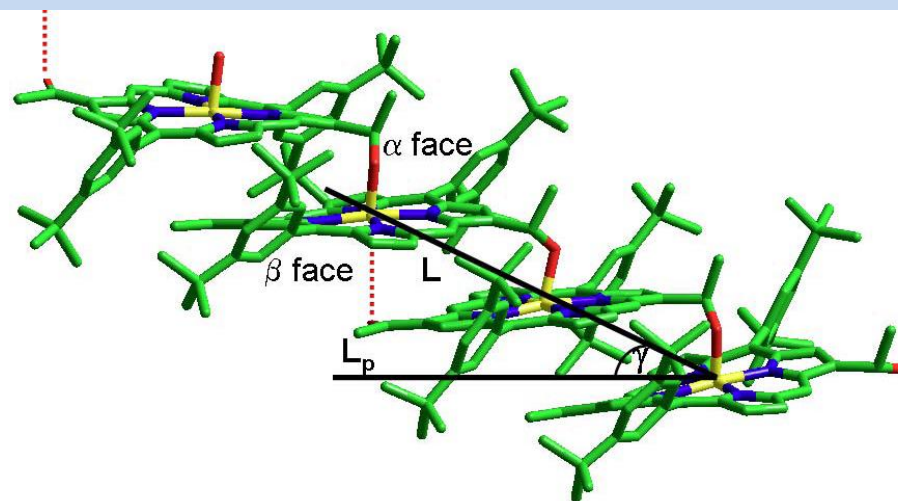
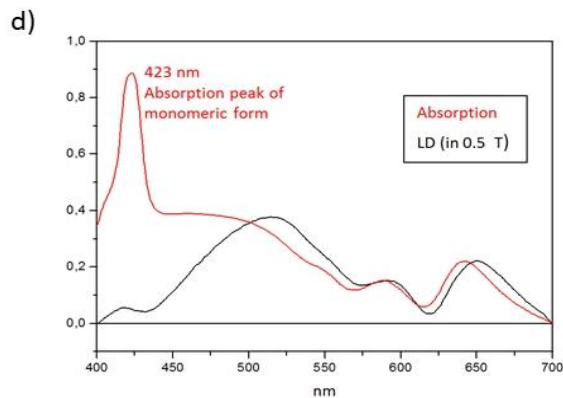
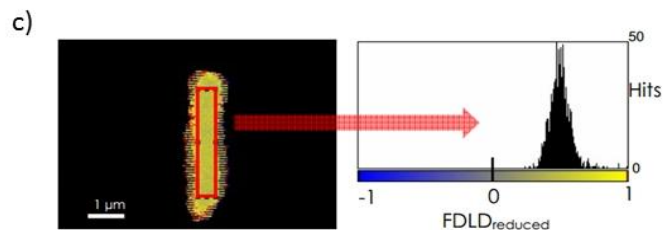
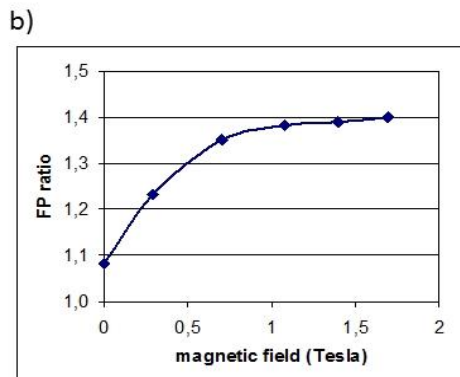
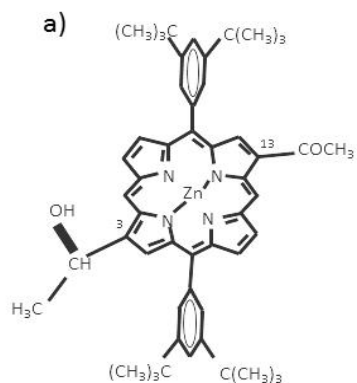
PEM

PEM controller

05.00 004880

KC 18	FT 510
OC 11	FT 540
OC 12	FT 560
OC 14	FT 580
KC 10	FT 600
KC 14	FT 640

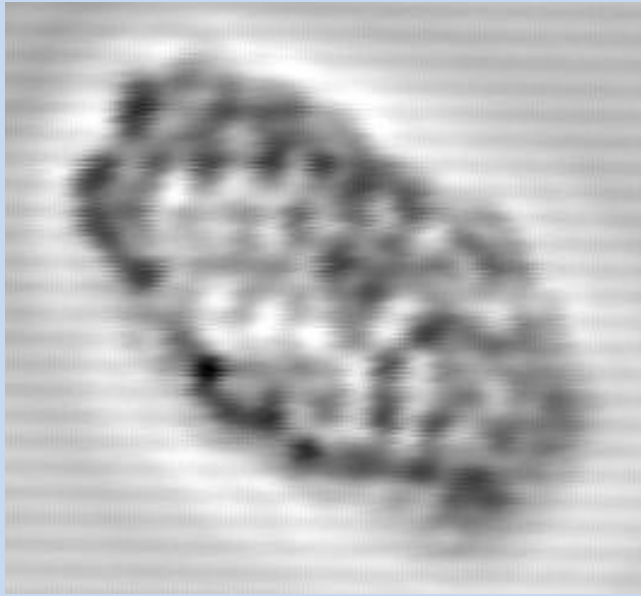
Artificial chlorosome



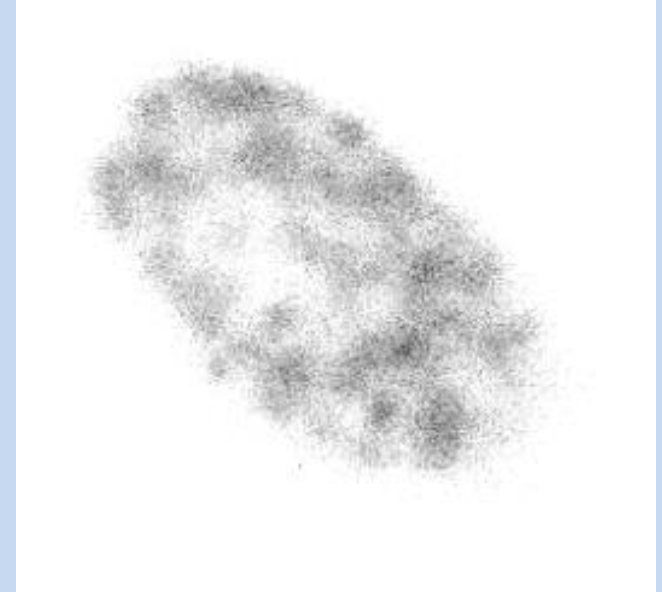
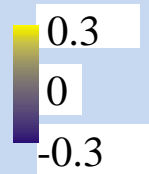
Orientation angles of the dipoles with respect to the long axes of the rods:

- ▶ Q_x $43^\circ \pm 8$ (SE:5.6)
- ▶ Q_y $37^\circ \pm 7$ (SE:0.42)
- ▶ B_x $39^\circ \pm 4$ (SE:0.73)

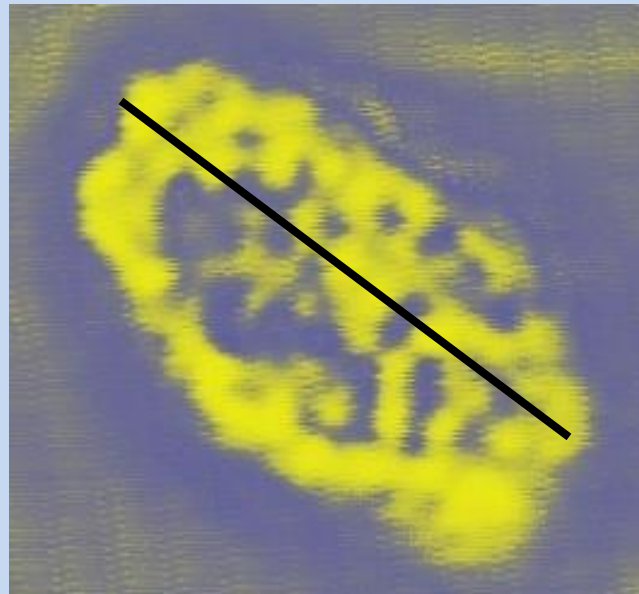
Birefringence of chloroplasts



Transmission

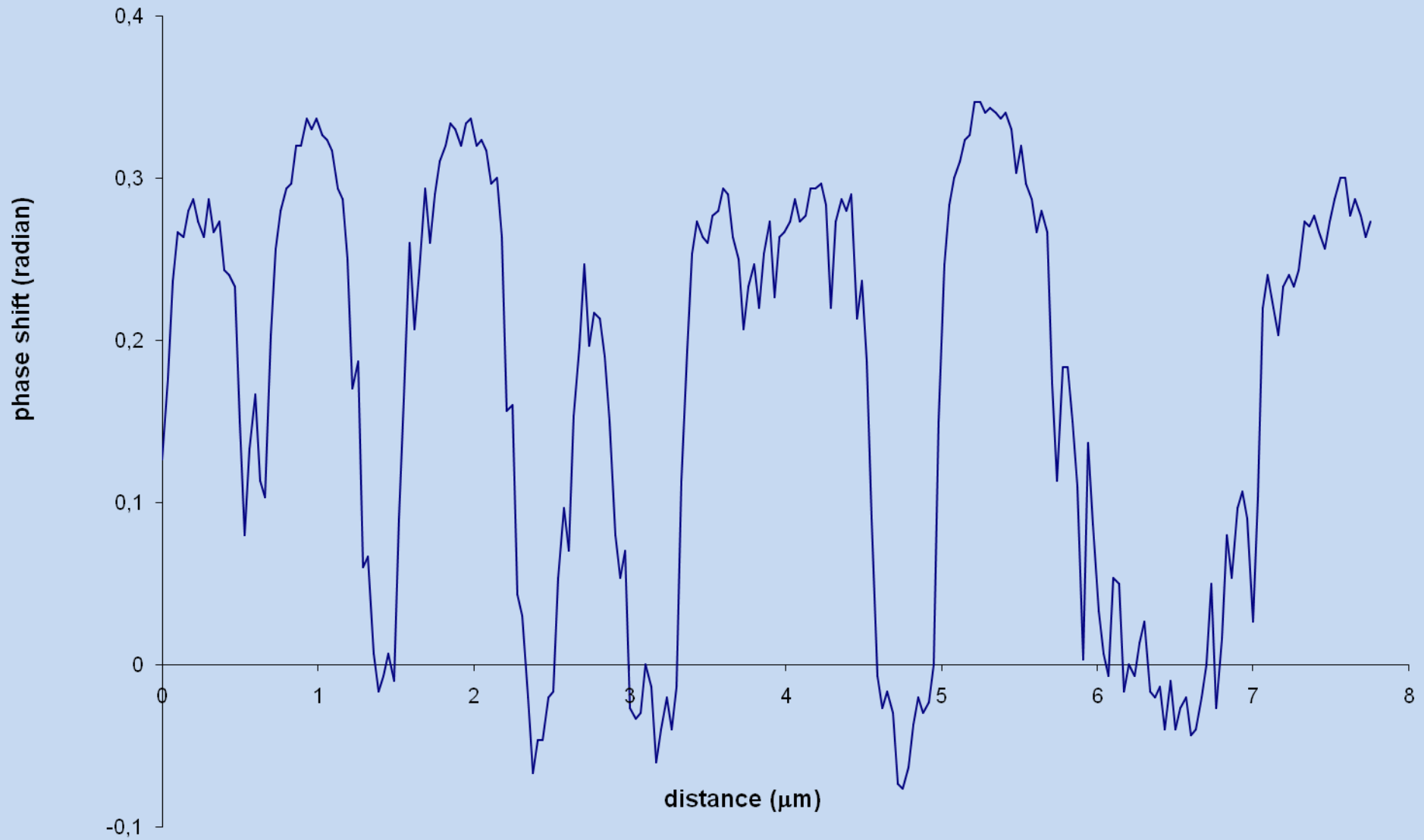


Fluorescence I



LB, linear birefringence

Values of LB (χ) along x



$$\tau_{lin} = -\frac{P}{\omega} \sin\left(2\pi \frac{R}{\lambda}\right) \sin(2\theta)$$

$$R = \Delta n \times d$$

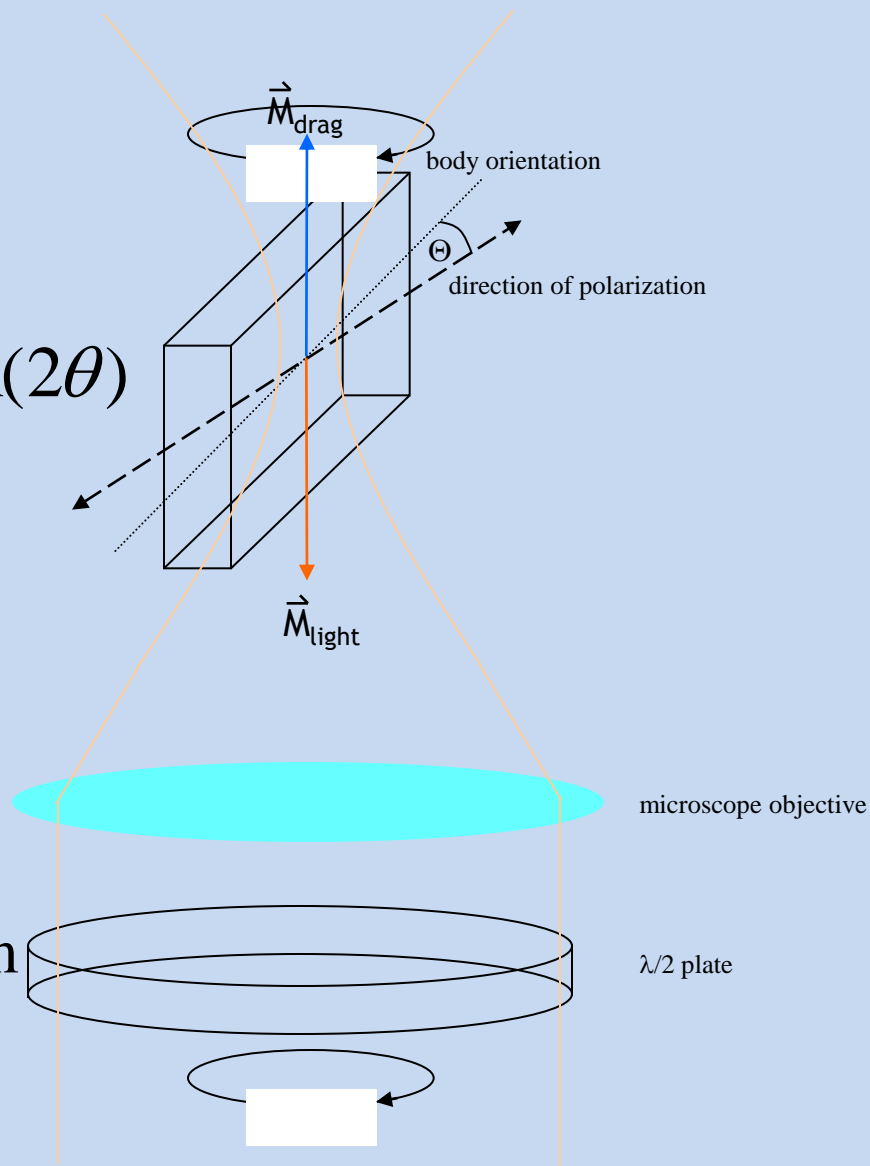
tau, torque

P, power of the laser beam

R, retardation

n, refractive index

d, thickness



Orientation (and rotation) of chloroplasts by (changing the plane of) linearly polarized beam of a laser tweezer

